



**Biomass Gasification with Carbon Dioxide-
Kinetic Studies**

Jhon Freddy Briceno Torres

Thesis to obtain the Master of Science Degree in
Energy Engineering and Management

Supervisors: Prof. Francisco Manuel da Silva Lemos
Prof. Wojciech Nowak

Examination Committee

Chairperson: Prof. Edgar Caetano Fernandes
Supervisor: Prof. Francisco Manuel da Silva Lemos
Member of the Committee: Prof. Carlos Manuel Faria de Barros Henriques

November 2018

To all the people who helped me during this time,

Thank you, from the bottom of my heart.

ACKNOWLEDGEMENT

I would like to appreciation to professors Amelia Lemos and Francisco Lemos, who were always helping me through the development of this study with their advices, guidance and the time that they took in order to let me achieve this goal.

Also, I'd like to thank Mr. Everton Santos, for his help and support during the laboratory experimentation.

I would like to thank InnoEnergy for letting me be part of this program in the Clean Fossil and Alternative Fuels master's and the 2 years that I have spent in the amazing countries of Poland and Portugal. I am grateful not only for the academic but also for the personal experience during the past years.

Finally, I would like to express my gratitude to all my family and friends for their time, support, advice, and availability for me during the past two years. Without them, it would have been very difficult to achieve this goal. To all of them, I will be grateful forever.

ABSTRACT

The current demand for energy in order to satisfy the human necessities is increasing every year. Today, the easiest way in order to fulfil this demand is with the use of fossil fuels, due to high availability and low price. But meeting this demand using fossil fuels has led to a series of environmental issues because these sources of energy have emissions that are harmful for the humanity and for the atmosphere. Giving an urgent solution to these problems has been a priority for the governments, who have started to see different solutions for alternative fuels that can lead to avoid having a dependence on fossil fuels. Biomass has turned into an interesting alternative in order to reduce the amount of emissions of greenhouse gases into the atmosphere

The main intention of this study is to make a kinetic study on the reactivity of a specific type of biomass, from eucalyptus, under different atmospheres including air, nitrogen, carbon dioxide, and different mixtures between air and carbon dioxide. The main interest was to analyze the behavior of the biomass degradation, the derivative weight, and the heating flow under different gasification conditions and under different heating rates (10, 20, 50 and 100 °C/min). Also, a kinetic model was developed to simulate each TG test and also a preliminary model was done to characterize the DSC heat flow measurements. The mass degradation models were developed assuming first-order reactions and restored to different pseudo-components to characterize the main components of the lignocellulosic biomass (Hemicellulose, cellulose and lignin).

The results showed good correlation between the models and the experimental data. A model was also developed to simulate the heat flow of each test. The correlation for these models was not as accurate as the kinetic models, but showed to be a promising route to follow.

Keywords: Biomass, gasification, pyrolysis, carbon dioxide, TGA, DSC, kinetics, heat flow.

RESUMO

A atual procura de energia para satisfazer as necessidades humanas está a aumentar de ano para ano. Hoje a maneira mais fácil de satisfazer essa procura é recorrendo à utilização de combustíveis fósseis, devido à sua elevada disponibilidade e baixo preço. Mas a utilização extensiva de combustíveis fósseis tem levado a uma série de problemas ambientais porque estas fontes de energia têm emissões que são prejudiciais para a humanidade e para a atmosfera. Dar uma solução urgente para este problema tem sido uma prioridade para os governos, que começaram a encontrar várias soluções, como combustíveis alternativos, que podem evitar ter uma elevada dependência dos combustíveis fósseis. A biomassa está a configurar-se como uma alternativa interessante para reduzir a quantidade de emissões de gases com efeito estufa para a atmosfera.

O objetivo principal deste estudo é fazer uma análise cinética da reatividade de um tipo específico de biomassa, a partir de eucalipto, sob diferentes atmosferas, incluindo ar, azoto, dióxido de carbono e diferentes misturas entre ar e dióxido de carbono. O interesse principal foi analisar o comportamento de degradação da biomassa, através da variação de massa, e a taxa de fluxo térmico sob diferentes agentes de gaseificação a diferentes velocidades de aquecimento (10, 20, 50 e 100 °C/min). Além disso, foi desenvolvido um modelo cinético para simular cada um dos testes de TG e também um modelo para caracterizar o comportamento de fluxo de calor observado pelo DSC. Os modelos de degradação assumiram reações de primeira ordem e utilizaram diferentes pseudo-componentes para caracterizar os principais componentes da biomassa lignocelulósica (celulose, hemicelulose e lignina).

Os resultados obtidos mostraram uma boa correlação entre o modelo e os resultados experimentais. Também foi desenvolvido um modelo para simular o fluxo de calor observado em cada um dos ensaios. A correlação para estes modelos de fluxo térmico não foram tão bons como para os modelos de variação de massa mas mostraram ser uma via interessante para continuar.

Palavras-chave: Biomassa, gasificação, pirólise, dióxido de carbono, TGA, DSC, cinética, fluxo térmico.

TABLE OF CONTENT

ACKNOWLEDGEMENT.....	3
ABSTRACT	4
RESUMO.....	5
LIST OF FIGURES.....	8
LIST OF TABLES.....	10
1. INTRODUCTION.....	11
1.1 Overview.....	11
1.2 Objective.....	12
2. THEORETICAL REVIEW	13
2.1 Biomass	13
2.1.1 Cellulose	14
2.1.2 Hemicellulose	14
2.1.3 Lignin	15
2.2 Biomass conversion routes	16
2.2.1 Combustion.....	16
2.2.2 Gasification	17
2.2.3 Pyrolysis	19
2.3 Factors affecting combustion, gasification and pyrolysis of biomass.....	20
2.3.1 Effects of particle size.....	21
2.3.2 Effects of heating rate.....	21
2.3.3 Temperature	22
2.3.4 Carrier gas	22
2.4 Kinetic modelling of biomass	23
2.5 Kinetic models for thermal mass degradation	26
2.6 Mathematical models for kinetic studies.....	27
2.6.1 Model-fitting method	28
2.6.2 Model-free methods (isoconversional)	28
2.7 Thermal analysis	29
2.7.1 Thermogravimetric Analysis (TGA)	29
2.7.2 Differential Thermal Analysis (DTA).....	30
2.7.3 Differential Scanning Calorimetry (DSC).....	31
2.8 Heat flow model.....	32
3. RESEARCH METHODOLOGY	33
3.1 Material	33
3.2 Equipment.....	33
3.3 Experimental method.....	34

3.4	Data processing and calculations.....	35
3.4.1	Biomass degradation analysis.....	35
3.4.2	Heating flow analysis.....	35
3.4.3	Curve model fitting calculations.....	36
3.4.4	Thermal model fitting.....	37
4.	RESULTS AND DISCUSSION.....	40
4.1	TGA/ derivative weight curve analysis	40
4.1.1	Pyrolysis.....	41
4.1.2	Combustion 100% air.....	42
4.1.3	Combustion 75% air- 25% CO ₂	44
4.1.4	Combustion 50% air- 50% CO ₂	46
4.1.5	Combustion 25% air- 75% CO ₂	47
4.1.6	100% CO ₂ gasification.....	49
4.2	Heat flow analysis.....	50
4.2.1	Pyrolysis.....	50
4.2.2	Combustion 100% air.....	51
4.2.3	Combustion 75% air- 25% CO ₂	52
4.2.4	Combustion 50% air- 50% CO ₂	53
4.2.5	Combustion 25% air- 75% CO ₂	54
4.2.6	100% CO ₂ gasification.....	55
4.3	TG vs DSC curve analysis.....	56
4.4	Specific heat of reaction analysis	58
4.5	Kinetic model fitting	60
4.5.1	Combustion and partial combustion models.....	60
4.5.2	Pyrolysis model	66
4.5.3	100% CO ₂ gasification.....	67
4.6	Heat flow model fitting	70
4.6.1	Oxidizing tests.....	70
5.	CONCLUSIONS AND RECOMMENDATIONS.....	73
5.1	Conclusions	73
5.2	Recommendations.....	75
6.	REFERENCES	78

LIST OF FIGURES

Figure 1. Global carbon emissions from fossil fuels on the 20 th century.[1].....	11
Figure 2. Cellulose chemical structure. [4]	14
Figure 3. Hemicellulose chemical structure.[8].....	15
Figure 4. Lignin chemical structure.[8]	15
Figure 5. Biomass processing technologies and products.[6].....	16
Figure 6. One step global model[29].	23
Figure 7. Competing model[29].	24
Figure 8. Broido-Shafizadeh model[31].	24
Figure 9. Complex competing model[30].	25
Figure 10. Complex Broido-Shafizadeh model[32].	25
Figure 11. Kinetics of isothermal degradation of wood [33].	26
Figure 12. Schematic of a thermobalance[44].	30
Figure 13. DTA curve[44].	31
Figure 14. DSC curve with positive endothermic trend[44].	31
Figure 15. SDT 2960 simultaneous DSC-TGA equipment with computer.	34
Figure 16. Derivative weight profile for pyrolysis test at 10°C/min heating rate.....	40
Figure 17. Biomass degradation profile and DTG curves pyrolysis at different heating rates.	41
Figure 18. Biomass degradation profile and DTG curves combustion 100% air at different heating rates.....	43
Figure 19. Biomass degradation profile and DTG curves combustion 75% air-25% CO ₂ at different heating rates.....	44
Figure 20. Biomass degradation profile and DTG curves combustion 50% air-50% CO ₂ at different heating rates.....	46
Figure 21. Biomass degradation profile and DTG curves combustion 25% air-75% CO ₂ at different heating rates.....	47
Figure 22. Biomass degradation profile and DTG curves Gasification 100 % CO ₂ at different heating rates.....	49
Figure 23. Heat flow DSC curves from Pyrolysis at different heating rates.	51
Figure 24. Heat flow DSC curves from Combustion 100% air at different heating rates.....	52
Figure 25. Heat flow DSC curves from combustion 75% air-25% CO ₂ at different heating rates.....	53
Figure 26. Heat flow DSC curves from combustion 50% air-50% CO ₂ at different heating rates.....	54
Figure 27. Heat flow DSC curves from combustion 25% air-75% CO ₂ at different heating rates.....	55
Figure 28. Gasification 100% CO ₂ DSC curves at different heating rates	56
Figure 29. TG and DSC curves for 100% air combustion (a.), and partial combustion of 75% air (b.), 50% air (c.) and 25% air (d.) mixtures at a heating rate of 10 °C/min.....	57
Figure 30. TG and DSC curves for pyrolysis (a.) and 100% CO ₂ gasification (b.) at a heating rate of 10 °C/min	58

Figure 31. Specific heat of reaction curve for 100% air combustion (a.), and partial combustion of 75% air (b.), 50% air (c.) and 25% air (d.) mixtures at a heating rate of 10 °C/min with compounds heats of formation.....	59
Figure 32. Biomass degradation profile of experimental and model information for air combustion at 10°C/min heating rate.....	60
Figure 33. Biomass degradation profile of experimental and model information for 75% air- 25% CO ₂ mixture at 10°C/min heating rate.....	61
Figure 34. Biomass degradation profile of experimental and model information for 50% air- 50% CO ₂ mixture at 10°C/min heating rate.....	61
Figure 35. Biomass degradation profile of experimental and model information for 25% air- 75% CO ₂ mixture at 10°C/min heating rate.....	62
Figure 36. Constant rate and activation energy for component 1 at different mixtures of air and CO ₂ .	63
Figure 37. Constant rate and activation energy for component 2 at different mixtures of air and CO ₂ .	64
Figure 38. Constant rate and activation energy for component 3 at different mixtures of air and CO ₂ .	64
Figure 39. Constant rate and activation energy for component 4 at different mixtures of air and CO ₂ .	65
Figure 40. Biomass degradation profile of experimental and model information for pyrolysis at 10°C/min heating rate.....	66
Figure 41. Biomass degradation profile of experimental and model information for CO ₂ gasification at a 10°C/min heating rate.....	68
Figure 42. Heat flow experimental and model data for 100 % air combustion at a heating rate of 20 °C/min.....	70
Figure 43. Heat flow experimental and model data for 75%air-25% CO ₂ mixture combustion at a heating rate of 50 °C/min.....	71

LIST OF TABLES

Table 1. Composition of cellulose, hemicellulose and lignin of a few types of biomass.[6]	14
Table 2. Characteristics of some pyrolysis processes[4].	20
Table 3. Proximate and ultimate analysis of material.....	33
Table 4. Pyrolysis highest derivative weight peak and temperature vs heating rate.	42
Table 5. 100% combustion highest derivative weight peak and temperature vs heating rate.	44
Table 6. 75% air- 25% CO ₂ highest derivative weight peak and temperature vs heating rate.....	45
Table 7. 50% air- 50% CO ₂ highest derivative weight peak and temperature vs heating rate.	47
Table 8. 25% air- 75% CO ₂ highest derivative weight peak and temperature vs heating rate.	48
Table 9. 100% CO ₂ gasification highest derivative weight peak and temperature vs heating rate.....	50
Table 10. Kinetic constants at reference temperature and activation energies for every pseudo component used in all of the oxidizing tests.....	63
Table 11. Model fitting quality parameters for all oxidizing tests. Square error residuals and correlation factor between experimental data and model data.	65
Table 12. Pyrolysis model fitting parameters for all heating rates.....	66
Table 13. Model fitting quality parameters for pyrolysis. Square error residuals and correlation factor between experimental data and model data.	67
Table 14. 100% CO ₂ gasification model fitting parameters for all heating rates	68
Table 15. Model fitting quality parameters for pyrolysis. Square error residuals and correlation factor between experimental data and model data.	69
Table 16. Air combustion heats of reaction model parameters for all heating rates with correlation factor.....	71
Table 17. 75%Air-25% CO ₂ combustion heats of reaction model parameters for all heating rates with correlation factor.	72
Table 18. 50%Air-50% CO ₂ combustion heats of reaction model parameters for all heating rates with correlation factor.	76
Table 19. 50%Air-50% CO ₂ combustion heats of reaction model parameters for all heating rates with correlation factor.	76
Table 20. Pyrolysis heats of reaction model parameters for all heating rates with correlation factor... ..	77
Table 21. CO ₂ gasification heats of reaction model parameters for all heating rates with correlation factor.....	77

1. INTRODUCTION

1.1 Overview

The current demand for energy in order to satisfy the human necessities is increasing every year. Today, the easiest way in order to fulfil this demand is with the use of fossil fuels, due to high availability and low price. However, meeting this demand using fossil fuels has led to an environmental issue because these kinds of energies are harmful for the humanity and for the atmosphere. The amount of CO₂ and other greenhouse gases on the atmosphere has increased exponentially during the last century and the statistics show that this trend will continue to grow.[1] Figure 1 shows the trend of the past century and how the carbon emission from fossil fuels has grown in an exponential manner on the past 70 years.

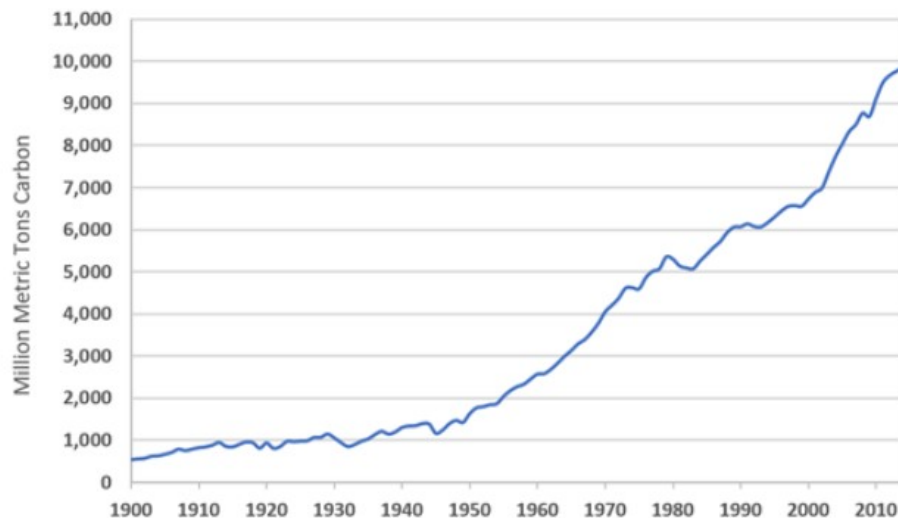


Figure 1. Global carbon emissions from fossil fuels on the 20th century.[1]

Giving an urgent solution to this problem has been a priority for the governments, who have started to see different solutions for alternative fuels that can lead to avoid having a dependence on fossil fuels. Biomass has turned into an interesting alternative in order to reduce the amount of emissions of greenhouse gases into the atmosphere. Biomass is known to absorb the solar energy in the photosynthesis process. This process involves the reaction of water and CO₂. When this material is used for combustion, the CO₂ that was absorbed is released back to the atmosphere, making the use of biomass as an energy source a carbon neutral process. Due to this feature, using biomass as a potential hydrocarbon replacement has become one of the paths to reduce carbon emissions, and studies have been increasing in the last period of time. Using the biochemical energy that is stored in the biomass is the main goal of the biomass-to-energy processes, which can be done either by thermochemical processes or biochemical processes. This study is related to the thermochemical conversion process, in which one specific type of biomass that is common in Portugal (Eucalyptus) will

be submitted to pyrolysis, combustion and gasification tests in order to make a kinetic analysis of the different processes involved, which include how much the biomass decomposition process changes with different processes under different carrier gases.

Other studies have been done in order to find alternative processes that can use CO₂ as a potential feedstock, and deal with the vast amount of streams that are emitted daily. The idea is to have a possibility to recycle part of the emitted stream and use it for other purposes. One type of studies that has been carried out is using CO₂ in the gasification processes as a gasification media. Several studies have been done using coal and some for biomass as a feedstock. For example, Ye et al.[2] made a study in which they used a low rank coal and made gasification tests with CO₂ and with steam, and found that the CO₂ gasification had lower activation energy when compared to steam, but the reactivity was higher. Marquez-Montesinos et al[3] used grapefruit skin char and made gasification experiments with steam and with CO₂. They also reported that the activation energy was lower with CO₂ when compared to steam, and that the reactivity was higher, due to a catalytic effect of minerals present on the biomass.

In this study, CO₂ will also be used as a gasification media for the tests, using pure CO₂, and also using mixtures of air and CO₂. The goal is to be able to compare how using CO₂ affects the kinetics of the biomass gasification, and also to see how the heat that is required for the operation is affected by the presence of this gas, and its respective mixtures. The use of CO₂ as a gasifying agent is relevant not only for CO₂ gasification but also for the full understanding of the process in a conventional gasifier.

1.2 Objective

The main objective of this project is to make a study of the thermochemical conversion of Eucalyptus biomass, in different oxidizing and non-oxidizing atmospheres, including: nitrogen, air, CO₂, and mixtures of air and CO₂, at different heating rates, with the objective of having a review on how the mass loss behaviour changes with respect of the atmosphere that is being used, and also, information about the kinetic parameters of these different behaviour changes with different atmospheres.

Also, a kinetic model was developed in order to describe the mass loss behaviour with single global reaction kinetics, which could predict the kinetic behaviour of the biomass when it was being subjected to different atmospheres. Finally, a heat flow model was done in order to simulate the heat flow of each test done using different atmospheres.

2. THEORETICAL REVIEW

2.1 Biomass

Biomass is a material that stores energy by photosynthesis process when the sun is present. It is also material coming from living organisms (plants, animals, crop residues). The overall composition varies significantly but it is composed in large amounts of carbohydrates, $C_6H_{10}O_5$ with some variations with different physical properties of biomasses. Biomass is considered as a clean energy due to the fact that during its life, it stores chemical energy as carbohydrates by combining solar energy and CO_2 in the photosynthesis. This CO_2 that was captured during its life is released in the combustion process. Biomass has become one of the most interesting forms of renewable energies of the present options that are available, as this is located almost all around the world and this can give a solution to the present energy dependence of fossil fuels (almost 80% of actual energy consumption), and that represents an environmental issue. Biomass has currently an important share of the global energy production with around 10-14%. [3]

There are 2 broad groups in which biomass can be divided[4]:

- Virgin biomass: Including plants, wood, leaves (lignocellulosic material), vegetables and crops.
- Waste biomass: Solid and liquid wastes (municipal solid waste), animal waste, human waste, sewage, gases derived from landfilling (methane), agricultural wastes.

Biomass is a mixture of carbohydrates, fats, proteins, with small quantities of minerals such as sodium, phosphorus, iron, calcium. The 3 main components of the plant biomass are: extractives, cell wall components, and ash. The extractives can be separated by treatment with solvents and recovered by evaporation of the solution. They include protein, oil, sugar and starch as the main components. The cell wall provides a structural strength to the wall. It is predominantly made of carbohydrates and lignin. Carbohydrates are mainly in the form of cellulose or hemicellulose fibers (imparting strength to the structure), that are held together by the lignin. The ash is mainly constituted by the inorganic part of the biomass. [4][5]

Lignocellulosic biomass is one of the most important types of biomass, as the major part of the biomass falls under this category. This is the nonstarch and fibrous part of the material , composed mainly by 3 components: Cellulose, hemicellulose, and lignin. The amount of cellulose, hemicellulose and lignin in a given biomass vary depending on the type of biomass, which makes it more or less interesting to be used as a feedstock for energy conversion. Table 1 shows some biomass types and their proportions of cellulose, hemicellulose and lignin. [4][5]

Biomass	Cellulose (%)	Hemicellulose (%)	Lignin (%)
hard			
wood	40-50	25-35	20-25
soft wood	40-50	25-30	25-35
flax	80	13	2
hemp	74,1	7,6	2,2
sugar			
cane	51,8	27,6	10,7
bamboo	54,6	11,4	21,7
pine	39,9	24,2	27,4
blue gum	41	19,4	28,1

Table 1. Composition of cellulose, hemicellulose and lignin of a few types of biomass.[6]

2.1.1 Cellulose

Primary structural component of the cell walls in the biomass. It has the general formula $(C_6H_{10}O_5)_n$, it's a long chain polymer with a high degree of polymerization and a high molecular weight. It has a crystalline structure, which gives it high strength, giving strength to the cell walls. The cellulose monomer is mainly D-glucose, made up from 6 carbons (hexose sugars). [4], [5], [7]

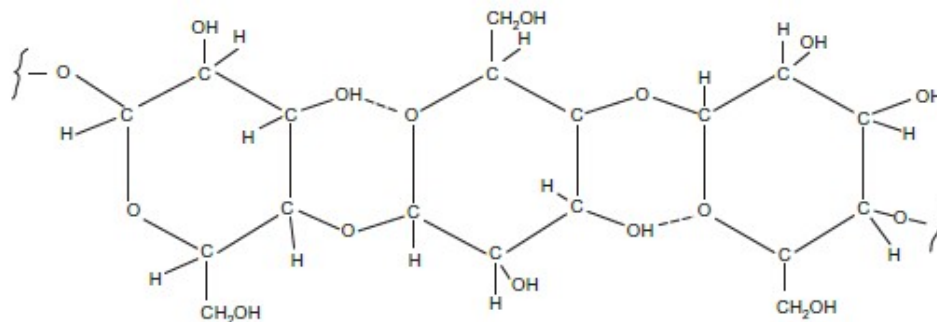


Figure 2. Cellulose chemical structure. [4]

2.1.2 Hemicellulose

Is another component of the cell walls of the biomass. The general formula is $(C_5H_8O_4)_n$, but, unlike cellulose, it has a random, and amorphous structure that has little strength. It is a carbohydrate polymer with a branch chain structure, and a low degree of polymerization. The detailed composition of hemicellulose varies between different biomass. Most of hemicelluloses are composed by sugar residues such as D-xylose, D-arabinose, D-glucose, D-mannose. Hemicellulose is soluble in weak alkaline solutions and it is hydrolyzed by a dilute base or acid. [4], [5], [7]

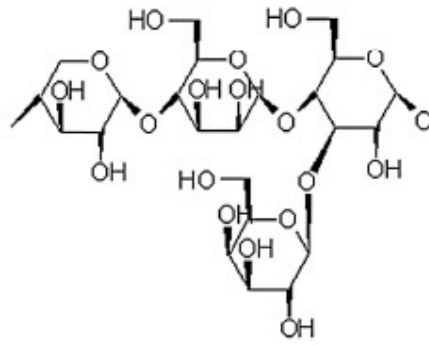


Figure 3. Hemicellulose chemical structure.[8]

2.1.3 Lignin

Lignin is a complex branched polymer mostly composed of phenylpropane moieties. It is a three dimensional polymer of 4-propenyl phenol, 4-propenyl-2-methoxy phenol, and 4-propenyl-2,5-dimethoxy phenol.[4] Lignin is in charge of joining together the cellulose fibers, holding adjacent cells one to each other. Lignin is highly insoluble, even in sulfuric acid.[4], [5], [9]

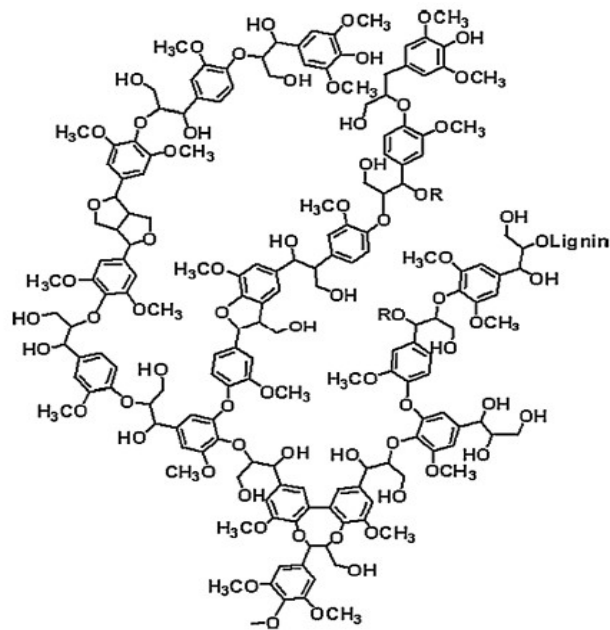


Figure 4. Lignin chemical structure.[8]

2.2 Biomass conversion routes

There are several technologies to convert biomass, which are divided into 2 main routes: thermochemical processing and biochemical processing. Thermochemical processes are the ones that expose the biomass to high temperatures and different oxidizing and non-oxidizing atmospheres (combustion, gasification, pyrolysis), in order to liberate the chemical energy that is contained in the biomass and transform it into electrical energy, heat, mechanical energy or chemicals. Biochemical processing uses microorganisms to break down organic material into more simple compounds (as methanol), chemicals, liquid and gaseous fuels[6]. Figure 5 shows different paths to obtain products.

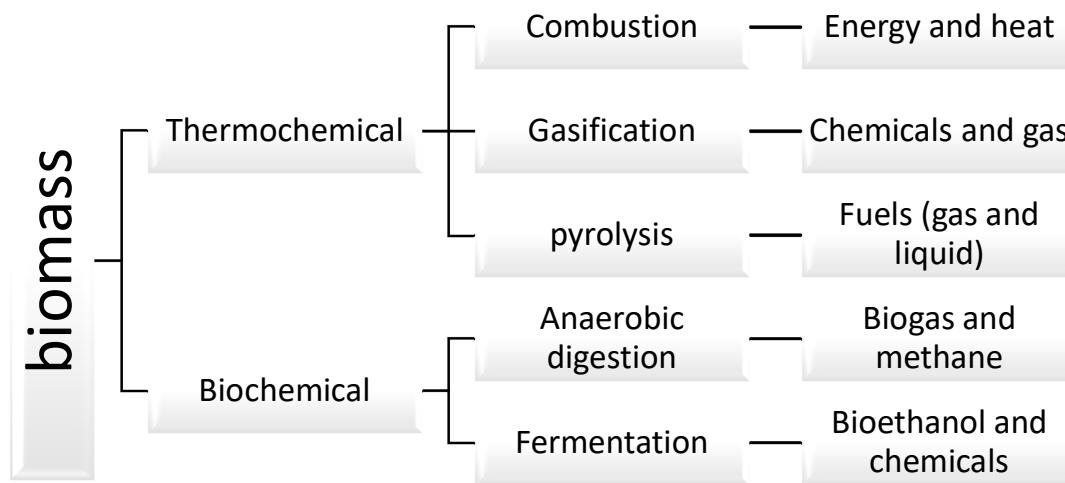
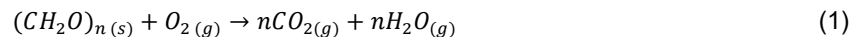


Figure 5. Biomass processing technologies and products.[6]

2.2.1 Combustion

In this process the biomass is exposed to high temperatures in an oxygen rich environment, which allows the biomass to totally oxidize to gases, ash, and residue. [10] This reaction produces mainly CO_2 and H_2O . This reaction is mainly exothermic and releases the chemical energy contained in the biomass in form of heat.



There are 3 different stages of combustion[10]:

- Pre-ignition: Solids are heated, dried, and partially volatilized.
- Flaming combustion of the vapor-phase volatiles and CO.
- Glowing (or smouldering) combustion of some char residue.

Initially the fuel is heated, and unbound water in the fuel evaporates. The thermal decomposition starts to occur in the heated fuel. In this stage, two non-oxidative reactions take place[10]:

- Primary volatilization of the cellulose substrate and secondary cracking of the volatiles to gas-phase fuels.
- Chemical dehydrations, decarbonylations, aromatization reactions, producing char, and gases such as CO and H₂O.

The second class of reactions is the flaming combustion, which is the oxidation of air in the hot gaseous products of volatilization. (Seen as visible light).

The third reaction is the combustion of char, involving solid-gas phase oxidation. Char combustion is incomplete in biomass fire because the charred residue cools below ignition temperature.

2.2.2 Gasification

Gasification is the thermochemical conversion of biomass (solid) into a combustible, in an atmosphere with a lower presence of oxidant agent (lower than stoichiometry, with 1.5:1 to 1.8:1 air to fuel ratio), in a gasifier (gasifying reactor). With this technology, it is possible to turn biomass into different liquid and gaseous fuels that can be synthesized to different products like power generation, electricity, transportation, etc. The main product from gasification is CO and H₂ which can be used to convert to synthetic natural gas (CH₄) by catalytic methanation of carbon monoxide (CO). A lot of feedstocks can be used, going from energy crops to wastes, such as industrial waste, agro waste, food waste, kitchen waste, and transformed to bioenergy to replace products derived from petrochemical industry. [11]–[13]

The stages that are part of the gasification process are the following:

- Drying zone.
- Pyrolysis (Thermal decomposition).
- Reduction zone.
- Partial oxidation (combustion zone).

Drying zone

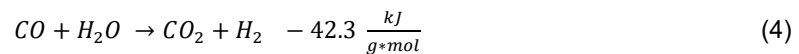
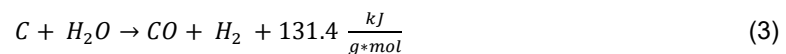
One of the most important characteristics of biomass is its moisture content, as it plays a vital role in the quality of the product. Biomass can have a different moisture content that typically varies from 5% to 35%. In this zone of the reactor, the typical temperature is around 100°C. The moisture content of the biomass is converted to steam, but the fuel that is present in the biomass does not undergo any significant thermal decomposition of the volatile matter. In this zone from a feedstock with moisture, the product is dry feedstock and water. [11]–[13]

Pyrolysis zone

Thermal decomposition in the absence of air. Process normally taking place between 125-500°C. The products released are liquid tars (from condensation of hydrocarbons), charcoal, and gases. The proportion is dependent on the biomass used and the operation conditions. Below 200° C the drying process is still taking place and also there is some reduction of the molecular weight of the constituents. At 300° C and higher temperatures, the amorphous cellulose present in the biomass starts reducing to form carbonyl, carboxyl group radicals, CO and CO₂. At temperatures beyond 300 °C the crystalline cellulose is decomposed into tar, char and gaseous products. Hemicellulose it's decomposed into a soluble polymer forming also volatile gases, tar, char. Lignin is decomposed at higher temperatures (300-500 °C) forming acetic acid, methanol, acetone, water among other compounds. For the chemical transformations that occur below 300 °C the reactions are exothermic, so there is no requirement for external heating. The chemical reactions that take place above 300 °C are usually endothermic reactions, and for the high temperature pyrolysis, heating is needed to maximize the yield (liquid or gas). [11]–[13]

Reduction zone

Gasification/pyrolysis also have byproduct forming, mostly undesired products such as NO_x (due to nitrogen content on air), SO₂ and tar contents, and this represents one of the biggest challenges in the utilization for power generation. It has been discovered that tar particles can be controlled setting an adequate temperature in the reduction zone, which is around 1000° C. In this zone, high temperature reactions are taking place in a reducing atmosphere, yielding conversion of charcoal and gases. This reduction is done while performing endothermic reactions to generate the combustible products, such as CO, H₂, and CH₄. Some of the reactions are: [11]–[13]



Combustion zone

Volatile materials from biomass oxidize under exothermic reactions. Typical temperature varies from 1100° C to 1500°C, and gaseous fuels are produced, for example, CO, CO₂, H₂, H₂O. In this stage the quality of the product is decided, by some of the key parameters (pressure, temperature, type of gasifying agents, like oxygen, air, etc.) For power purposes, oxygen is recommended as a gasifying

agent. Solid carbonized fuel and oxygen in air produce carbon dioxide and heat. Hydrogen is also combined with oxygen to produce water vapor [5]. The reactions are:[11]–[13]



2.2.3 Pyrolysis

Pyrolysis process is the thermal decomposition in the total absence of oxygen at high temperatures. This process decomposes the biomass, in which large hydrocarbon molecules are broken into smaller compounds, producing gaseous fuels, and some of them condense producing liquid fuels. The solid that remains is called biochar, and it is mainly composed of unreacted lignin and non-condensable gases. There are 4 stages of pyrolysis[4][14]:

- Drying
- Initial stage
- Intermediate stage
- Final stage

Drying stage

This stage is up to temperatures of 100 °C. In this stage the biomass loses free moisture and bound water. This moisture is converted to steam, but the fuel that is present does not undergo any thermal decomposition of volatile matter.[4]

Initial stage

This stage takes place between 100 to 300 °C. In this stage the exothermic dehydration and decarboxylation of the biomass occurs, with the release of water and low molecular weight gases, such as CO and CO₂. [4]

Intermediate stage

This stage occurs between 200-600 °C. This is known as primary pyrolysis. Most of the vapor and the bio oil are produced. Large biomass molecules are decomposed into char, condensable gases (vapors and precursors of liquid yield) and non-condensable gases.[4]

Final stage

This stage occurs between 300-900 °C. In this stage, there is a secondary cracking of volatiles into char and non-condensable gases. If the biomass is submitted to high temperatures long enough, the large-molecular-weight condensable gases could crack, having additional char and gases.[4]

Depending on the heating rate, the pyrolysis can be divided into 2 main types[4]:

- Slow pyrolysis
- Fast pyrolysis

Slow pyrolysis

The slow pyrolysis occurs when the time that is required to heat the fuel to the pyrolysis temperature is longer than the pyrolysis reaction time. In this process, the production of charcoal or char is the main interest. The biomass is slowly in the absence of oxygen at a low temperature (around 400 °C) for an extended period of time, which can be from minutes until days. This type of pyrolysis is divided into 2 types: Carbonization and torrefaction. While torrefaction uses a narrow temperature range (200-300 °C), carbonization uses a much higher range of temperature.[4]

Fast pyrolysis

Fast pyrolysis occurs when the time that is required to heat the fuel to the pyrolysis temperature is shorter than the pyrolysis reaction time. For fast pyrolysis, the production of liquid or bio-oil is the main interest. In this, the biomass is heated in a high speed, so that it reaches the peak temperature before it decomposes. The residence time is on the order of seconds or even milliseconds. The heating rate is high, going to speeds as 1000-10000 °C/sec. If the production of bio-oil is the main interest, the temperature should not exceed 650 °C. There are 2 main types of fast pyrolysis: flash and ultrarapid. [4]

Table 2 presents characteristics of different processes and the products that come from different pyrolysis types.

Pyrolysis type	Residence time	Heating rate	Final temp. (°C)	Products
Torrefaction	10-60 min	Very small	280	Torrified biomass
Carbonization	days	Very low	> 400	Charcoal
Fast	< 2 secs	Very high	500	Bio-oil
Flash	< 1 sec	High	< 650	Bio-oil, chemicals, gas
Ultrarapid	< 0.5 sec	Very high	1000	Chemicals, gas
Vaccum	2-30 sec	Medium	400	Bio-oil
Hydropyrolysis	< 10 sec	high	< 500	Bio-oil
Methanopyrolysis	< 10 sec	high	> 700	Chemicals

Table 2. Characteristics of some pyrolysis processes[4].

2.3 Factors affecting combustion, gasification and pyrolysis of biomass

There are several factors that affect the biomass product yield, and among all there are:

- Particle size
- Heating rate
- Temperature
- Carrier gas

2.3.1 Effects of particle size

The structure of the biomass (composition, size, shape) has an influence on the reaction, having an effect on the heating rate. If the biomass has a smaller particle size, it will have a smaller resistance to the escape of the condensable gases, which will escape to the surroundings before having a secondary crack. This will result in a higher yield in liquid. Bigger particle size, will facilitate secondary cracking as the gases have a bigger resistance to escape of the primary pyrolysis[4][5].

Gomez et al. [15] found that the grain size had an influence in the distribution of the products of the biomass pyrolysis and on the calculation of the reaction kinetic parameters. This is because of secondary reactions of the volatiles inside the solid matrix will change with the grain size. Montoya et al.[16] found that small particles are better for high heating rates, uniform distribution of temperatures and higher yields in bio-oil production. Larger particles decrease biomass conversion, and bring char formation. Shen et al.[17] made pyrolysis tests with oil mallee woody biomass, using 8 different particle sizes (0.18-5.6mm), pyrolyzing up to a temperature of 500 °C. It was found that the yield of bio-oil decreased as the average biomass particle size was increased from 0.3 to about 1.5 mm. Asadullah et al.[18] found that particle size of biomass has an important role in char structure at fast heating rate ($> 1000^{\circ}\text{C/s}$) pyrolysis, but it had no effect on char structure at slow heating rate pyrolysis (0.17°C/s).

2.3.2 Effects of heating rate

Heating rate places an important role on the yield and the composition product. For example, heating rapidly to a moderate temperature ($400\text{-}600^{\circ}\text{C}$) will yield more condensable gases, which will give a higher yield of liquids, while a slow heating rate to the same temperature will yield a higher amount of char.[4], [5] The residence time in the reactor is also important. During a slow heating rate, a gradual removal of volatiles allows a secondary reaction to occur between the char and the volatiles, having a secondary char formation. If a liquid yield is wanted, a high heating rate is preferable, with a moderate final temperature ($450\text{-}600^{\circ}\text{C}$), and a short gas residence time. If a gas production is wanted, a moderate to slow heating rate is better, with a high final temperature ($700\text{-}900^{\circ}\text{C}$), and a long gas residence time.

Chen et al.[19] made a pyrolysis test using poplar wood, at different temperatures and heating rates. It was concluded that increasing the heating rate promoted the generation of CO and CH₄, and also enhanced the carbon content of biochar, while decreasing the water content of bio-oil. Barneto et al. [20] studied the effects of heating rate on 2 different biomasses. It was found that a slow heating rate

produces more hydrogen than a fast heating rate. This could be related to the reactivity of the char produced in the first stage of the gasification process. Cetin et al. [21] studied the effects of pyrolysis pressure and heating rate on radiate pine char. In this study, it was concluded that with high heating rates the char particles melted. Also, the produced chars had less micropore network, because of melting. Williams et al.[22] made a study of slow pyrolysis of pine wood changing heat rates from 5 to 80 °C/min. It was found that as the heating rate was increased from 5 °C/min to 80 °C/min, there was a shift to higher values of temperature values for the maximum rate of weight loss.

2.3.3 Temperature

The temperature plays a determinant role in the process, as it affects the composition and the yield of the products. For example, for pyrolysis, the amount of char that is created depends on the temperature. If the process occurs at lower temperatures, the product will have a greater amount of char. The volatile content increases with higher temperatures. Also, the amount of non-condensable gases (CO, CO₂, H₂, CH₄) increases with temperature.[4], [5]

Demirbas[23] made a study of agricultural waste, such as olive husk, corncob, or tea waste, and investigate how did different conditions such as temperature or particle size affected product yields. He found that when the pyrolysis temperature increased, the bio-char yield decreased. At low temperatures, and low heating rates, there was a maximization of the bio-char yield. Zhang et al[24] studied the effects of pyrolysis temperature and heating time on the yield obtained from straw and lignosulfonate. They found that as the temperature increased, the biochar yield, volatile matter, hydrogen, oxygen, nitrogen and sulfur content decreased. On the other side, the pH, and carbon content increased as the temperature increased. Balas et al.[25] made experiments investigating the effects of temperature and pressure on gas composition and low calorific value on a fluidized bed reactor. It was found that the temperature in the fluid bed does not effect on the final composition of the gas, but the temperature on the freeboard has a direct impact, as for higher temperatures will increase the proportion of CO and H₂, a decrease in CH₄ and CO₂, and an increase in the lower calorific value of the gas.

2.3.4 Carrier gas

Gasification agent affects the yield of products, as using different gases can help to promote different chemical reactions that will change the yield of products and the carbon conversion. Using different gasifying agents, such as H₂O, CO₂, air, or a mixture between them, will change the final composition of the gases produces and tars.

Butterman et al.[26] studied the gas evolution, mass decay behavior and energy content of several biomasses and agricultural waste, doing steam and CO₂ gasification using thermogravimetric analysis and gas chromatography. It was found that carbon conversion was complete with 25% CO₂-75% steam mixture, compared to 90% conversion with pure steam in the temperature range of 800-1000°C. With 0-5% CO₂, there was an increase of CO concentration by a factor of 10, and a decrease in H₂ by a factor of 3.3 at 900 °C. Also, 100% CO₂ did a separation of cellulose from lignin at 380 °C in

a 1 °C/min heating rate. The CO₂ has the ability to enhance the pore structure, providing an access for the CO₂ to gasify the solid. Jeremias et al.[27] used steam and CO₂ as a gasification agent for wood chips in a spouting fluidized bed. It found that mixtures of CO₂ and H₂O in the gasifying agent improves char conversion, and that the combined agents were effective decomposing the tars when lime based materials were used in the fluidized bed. The gasifying agents composed by a mixture of H₂O and CO₂ led to higher conversions of char to gas, and the tar was decomposed as well. Cheng et al.[28] studied the behavior of CO₂ gasification of biomass (woodchips) in a fluidized bed. They found that when the CO₂-to-biomass ratio was increased, the mole fraction of CO in the producer gas increased, while the fraction of H₂ and CO₂ decreased. When the CO₂ percentage was in 60%, the fractions of CO and CH₄ in the producer gas were maximum, as well as the lower heating value, having the optimal condition. The moisture content and the particle size of the woodchips had a negative effect on the gasification performance, reducing the low heating value, cold gas efficiency and CO₂ conversion ratio.

2.4 Kinetic modelling of biomass

Biomass thermal decomposition is a complex process that involves several parallel reactions. To describe the behavior of the thermal decomposition, several studies have been done in order to develop mathematical equations that can predict a particular behavior. There have been studies that have considered from simple models with a simple one reaction model, until more complex models that uses several equations. These models are normally empirically based on the thermal decomposition behavior, and use several assumptions, depending on the complexity of the model. The following are some models that are used normally.

One step global model

Most simple model. It was used in the early stages of modelling. This was used in pyrolysis process, and it models it as a single step first order reaction. The biomass decomposes into volatiles and char[29].

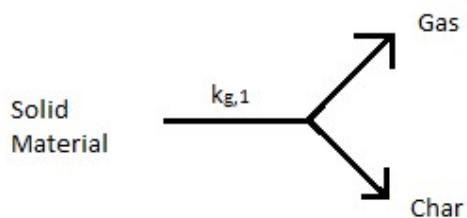


Figure 6. One step global model[29].

The main restriction that this model has is that the global reaction does not allow to describe how the hemicellulose, cellulose and lignin decomposes at their own temperatures.

Multi-reaction models

This type of model considers series of parallel or series multi-step reactions. There are several different models that have been proposed to explain the degradation of the biomass. A few will be explained next:

Competing model: This model was presented by Thurner et al[30]. The model features a changing char yield. There are 3 products that are being yielded: Gas, char, and tar. They assumed that the activation energies for the char-formation reactions were the same as the one for the weight-loss reactions. This ended with a final weight that is independent of the pyrolysis temperature.

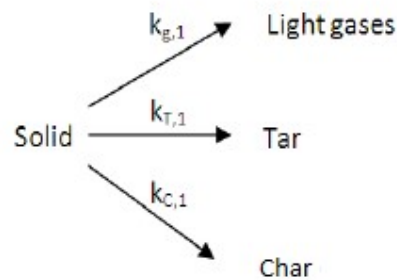


Figure 7. Competing model[29].

Broido-Shafizadeh: Kilzer et al[31]. Provided a model in which first the cellulose takes part in a reaction 1 in which the water is lost, having a new compound called dehydrocellulose, followed by a depolymerization of the unreacted cellulose (reaction 2) which volatilizes and form tars, and a final stage with decomposition of the dehydrocellulose to form a series of gases and char (reaction 3).

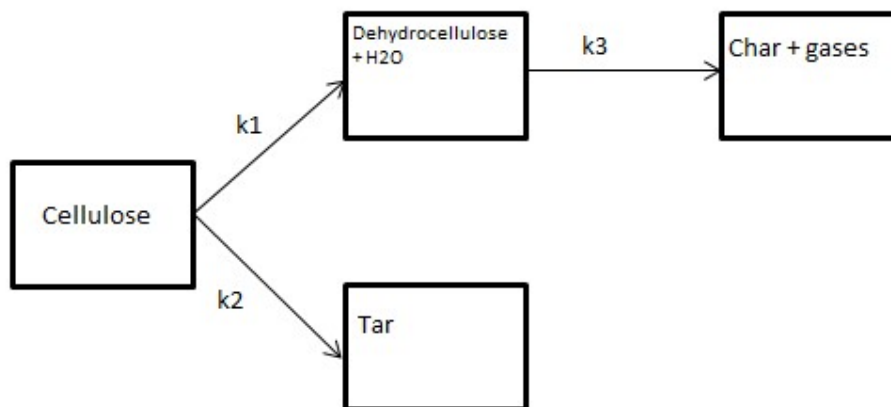


Figure 8. Broido-Shafizadeh model[31].

Complex competing model: The competing model was developed by Thurner et al[30], who added tar cracking and repolymerization reactions, in which the tar is decomposed into lighter gases or is polymerized in exothermic reactions. The primary reactions are assumed as first order reactions, having an Arrhenius type of temperature dependence. The secondary reactions are occurring on the gas/vapor phase within the pores of the solid matrix.

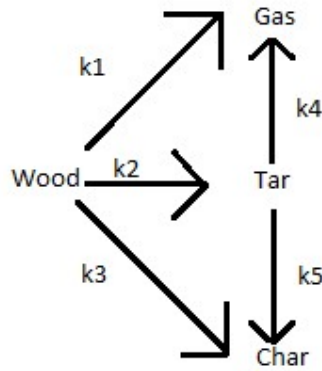


Figure 9. Complex competing model[30].

Complex Broido-Shafizadeh: Varhegyi et al[32] stated that the partial reaction in the intermediate step is actually a group of reactions that are taking place in this moment. k_0 , k_1 and k_2 are constants for reactions 0, 1 and 2. Reaction 0 is the non-catalyzed decomposition of cellulose. Reaction 1 is hydrolysis of cellulose in presence of water. Reaction 2 is the secondary reaction of the intermediates.

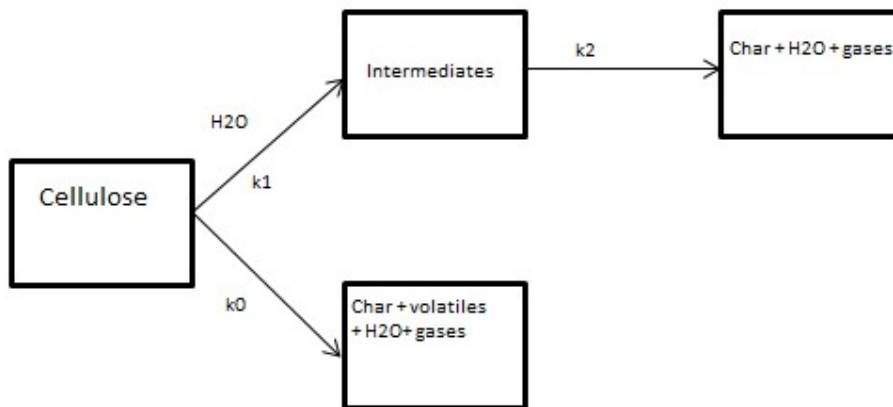


Figure 10. Complex Broido-Shafizadeh model[32].

Branca- Di Blasi model: Branca et al[33] made a study for the kinetics of thermal degradation of wood. They found that this mechanism fitted the experimental data:

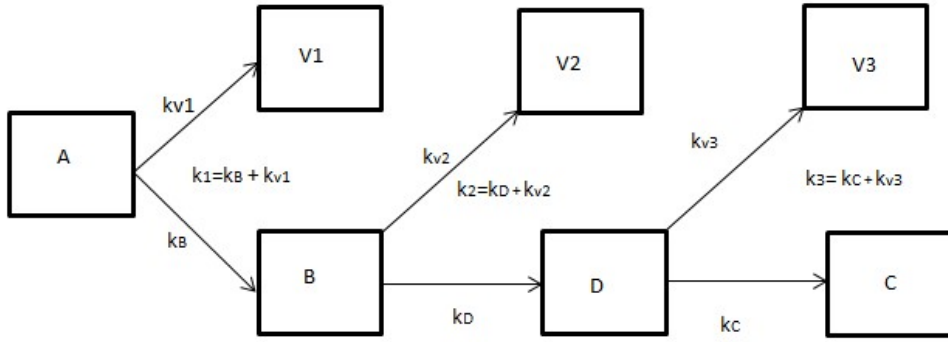


Figure 11. Kinetics of isothermal degradation of wood [33].

In the figure11, A is wood, B and D are intermediate products, V1, V2 and V3 are volatiles generated during the thermal decomposition and C is the char residue. These reactions follow an Arrhenius dependance on temperature and linearly dependent on the mass of the reactants A, B and D.

2.5 Kinetic models for thermal mass degradation

The thermal degradation of the biomass as a function of the temperature is often described by equation (8):

$$\frac{-dw}{dt} = k(T) * f(w) \quad (8)$$

Where w is the conversion (mass degradation), and k(T) is the reaction rate, which is given by the Arrhenius equation.

$$k(T) = A * e^{\frac{-E}{R} * \left(\frac{1}{T_n} - \frac{1}{T_{ref}} \right)} \quad (9)$$

Where:

A= Pre exponential factor. $\left(\frac{1}{min} \right)$

E_a = Activation Energy $\left(\frac{cal}{mol} \right)$

T_n = Experiment temperature at instant n. (K)

T_{ref} = Reference temperature. (K)

R= Universal gas constant. $\left(1.987 \frac{cal}{K * mol} \right)$

The main objective of the simulation is to calculate the activation energy, the reaction constants and the reaction model $f(w)$.

Commonly used models

There are different models that take into account structural changes in the solids during the reactions, some models have been proposed, such as [34]:

Volume reaction model (VRM): Simplest model, in which assumes that there is a uniform gas distribution in the entire particle, making the gas to react homogeneously with the char. This model was proposed by Ishida et al. [35]. The kinetic equation is:

$$\frac{dX}{dT} = k_v * (1 - X) \quad (10)$$

Changing grain size model (CGSM): This model was proposed by Georgakis et al. [36]. In this model, the char is composed by uniformly sized grains, with an ideal shape (spherical shape). The reaction rate is expressed as:

$$\frac{dX}{dT} = \left(\frac{3}{\tau}\right) * (1 - X)^{\frac{2}{3}} \quad (11)$$

$$\tau = \frac{r_g}{bv_b k_{CGSM} C^n} \quad (12)$$

$$r_g = \frac{3}{S_{BET} \rho_t} \quad (13)$$

This model uses τ which is a characteristic of the model, and also uses the initial grain radius r_g , which was calculated from the solid surface area.

Random Pore Model (RPM): Proposed by Bhatia et al. [37]. This model let arbitrary pore size distributions in the solid and overlaps pores surfaces. The reaction is expressed as:

$$\frac{dX}{dt} = \frac{k_{rpm} C^n S_0}{(1 - \epsilon_0) \rho_M} (1 - X) \sqrt{1 - \psi \ln(1 - X)} \quad (14)$$

$$\psi = \frac{4\pi L_0 (1 - \epsilon_0)}{S_0^2} \quad (15)$$

ψ is a characteristic of the model presented. This model requires to have the data of porosity ϵ_0 , surface area, surface area S_0 , and pore length L_0 of the solid porous system.

2.6 Mathematical models for kinetic studies

Experimental studies have been made for studying the kinetic reactions of the biomass degradation, which can be made isothermally and non-isothermally. There are two main categories in which the mathematical methods can be divided, which are model-fitting methods and model-free methods (isoconversional).

2.6.1 Model-fitting method

In this method, the model is fitted into the data, until the best statistical approach is achieved. From this, the activation energy (E_a) and the pre-exponential factor (A) is calculated. This type of approach is commonly used in pyrolysis reaction studies. A set of kinetic parameters is presented for a range of temperatures and a reaction, and this is called apparent kinetic parameters. For this method there are isothermal and non-isothermal approaches.

Isothermal: This method has 2 main options: It can determine the rate constant of the model (k) from the model that fits the best the experimental data, or can determine specific parameters like activation energy (E_a) or pre-exponential factor (A) using the Arrhenius equation, with experiments at different temperatures.

Non-Isothermal: This method provides the data for activation energy (E_a), pre-exponential factor (A) and model from non-isothermal data. For this method, there are some assumptions that are taken into account:

1. The A , E_a and model are constant (known as kinetic triplet).
2. They fit the 3 parameters for a single run, sometimes this is not good enough to provide the reaction kinetics.

Nedelchev et al.[38] made a review of the basic methods for non-isothermal analysis, and also made a study of kinetics of non-isothermal decomposition of calcium carbonate. Abbasi et al. [39] made an examination on the reliability on the of the kinetic parameters of the Coats-Redfern (CR) equation. They simulated TGA curves for reactions with different kinetic models, and found that the characteristics of CR approach to kinetic analysis of TGA data are unsuitable for determination of kinetic parameters. Garrigos [40] made a kinetic study of biomass modelling for combustion and pyrolysis. She found the kinetic parameters for 5 different type of biomasses under oxidizing and non-oxidizing atmospheres at 4 different heating rates. Pokwizcal [41] made a study for thermochemical conversion of wooden chips, getting the kinetics information under different temperatures and carrier gases. Finally, a gasification simulation was done for the results obtained.

2.6.2 Model-free methods (isoconversional)

These methods calculate the activation energy (E_a) by a series of experiments at different heating rates. This is done by grouping terms like the pre-exponential factor (A) and model into the intercept of a linear equation, and using this slope to calculate the activation energy (E_a). This model only reports activation energies (E_a).

Isoconversional methods are model-free that can be used to evaluate kinetic parameters, activation energy (E_a) and conversion (X), but require several kinetic curves for the analysis to be performed. For a same conversion value, calculations are done at different heating rates. This method evaluates

the activation energy for each conversion point (E_a , X). These model free methods also analyze isothermal and non-isothermal data.

Friedman[42] developed an isothermal method to obtain kinetic parameters to describe the thermal degradation of plastics from TGA data, based on the inter-comparison of experiments done at different linear heating rates, being able to determine the activation energy (E_a) without an explicit form for the kinetic equation.

Kissinger[43] presented a non-isothermal method, in which he constructed curves of reaction rate vs temperature for constant heating rates by analytical methods, that were used to demonstrate the effect of varying the order of reaction. The results of his study were congruent with results presented with isothermal methods.

2.7 Thermal analysis

The thermal analysis is the main technique that is being studied in this document, and the following techniques will be presented in this study:

- Thermogravimetric Analysis (TGA)
- Differential Thermal Analysis (DTA)
- Differential Scanning Calorimetry (DSC)

2.7.1 Thermogravimetric Analysis (TGA)

This type of study is done in order to analyze the change of weight of a sample as a function of time and temperature. This is done in a controlled environment, so the nature and the pressure of the atmosphere surrounding the sample can be controlled.[44] This type of measurements is done for material characterization and to evaluate the thermal stability of a sample. The materials can lose weight due to oxidation, dehydration or material degradation. Figure 12 shows a schematic of a thermobalance.

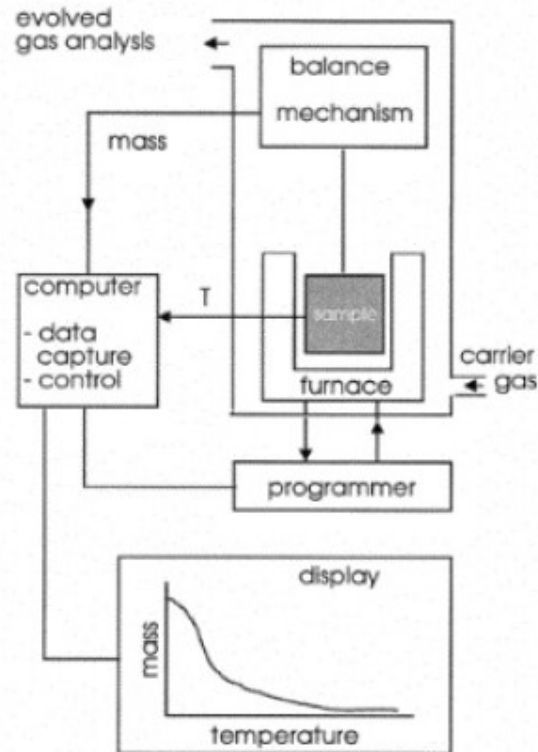


Figure 12. Schematic of a thermobalance[44].

The applications of this technique are: composition of components, thermal stability, degradation kinetics, moisture and volatile content of materials.

2.7.2 Differential Thermal Analysis (DTA)

In this technique, the difference in temperature ΔT , is measured between a sample and the reference material while they both are exposed to a same heating program[44]. When there is thermal event taking place in the material being tested, there will be a difference in temperature between the sample temperature and the reference temperature. For example, if it's an endothermic process, the temperature of the sample will fall behind the temperature of the reference. For an exothermic process, it will be on the opposite direction. The output that comes from this process is similar to the graph that is shown on figure 13. For this DTA curve, it has to be marked with the endo or the exo direction.

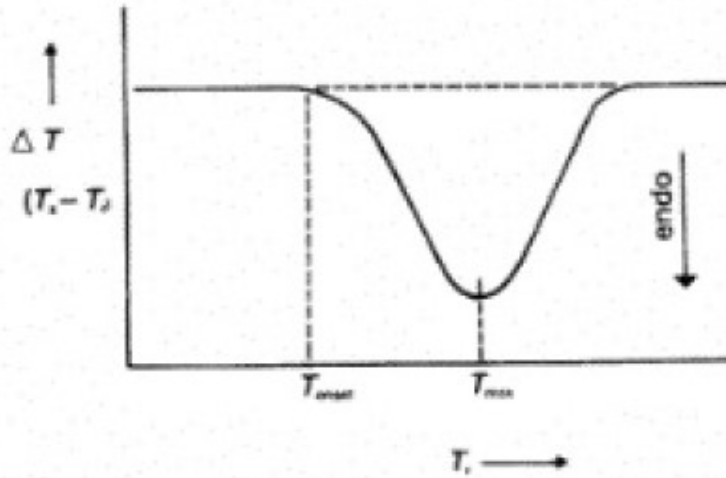


Figure 13. DTA curve[44].

2.7.3 Differential Scanning Calorimetry (DSC)

In this method, the sample and the reference material are maintained at the same temperature during the experiment. The difference in enthalpy from the sample and the reference are recorded against the recorded temperature[44]. The data is recorded as thermal deviations from the baseline, either if it's endothermic or exothermic, depending on if there was more or less energy supplied to the sample compared to the reference. These directions are marked on the record. For some equipment, the endothermic procedure is seen as positive, for other, this is shown as negative. On figure 14, an example is shown with a positive endothermic behavior.

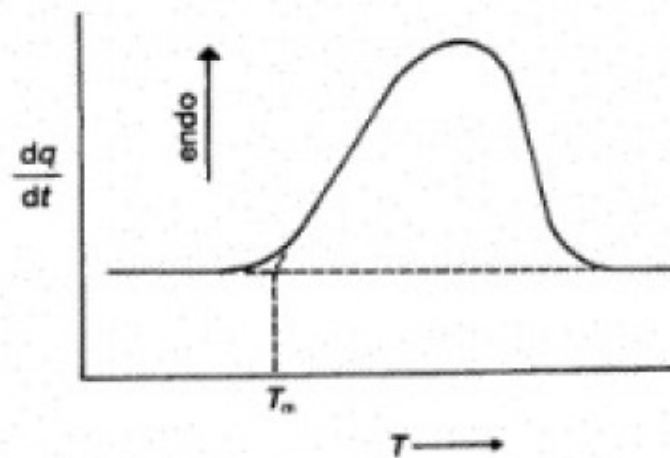


Figure 14. DSC curve with positive endothermic trend[44].

2.8 Heat flow model

The heat flow model is done in base on the change of enthalpy of the reaction:

$$\frac{dQ}{dt} = m_{react} * cp_{react} * \Delta T + \frac{dw}{dt} * H_{reaction} \quad (16)$$

Where:

m_{react} : mass of reactant.

cp_{react} : Specific heat reactant.

ΔT : Temperature interval.

$\frac{dw}{dt}$: Derivative weight

$H_{reaction}$: Enthalpy of reaction.

The main objective is to find the values of the C_p , and the enthalpy of the reactions that can be used with the masses of products and reactants that were calculated in the TGA to simulate the heat of reaction that was acquired during the experiments.

Haseli et al.[45] made a model to find kinetic parameters, particle pyrolysis and heat of reactions (temperature dependent) for a type of biomass. They took in account for variations the heat of reaction with the temperature, using 3 parallel reactions yielding gas, char and tar. Their model showed that the sensible heat released because of the biomass was responsible for the description of some experimental observations. Koufopoulos et al[46] provided a model that describes the pyrolysis of a single solid particle of biomass . Their thermal properties in the model are linear functions of temperature and conversion, and were fitted with experimental data. The heat of reaction was represented by 2 values: endothermic (prevailing at low conversions), and exothermic (prevailing at high conversions). The pyrolysis was simulated with 2 parallel reactions and a third reaction for the secondary reactions between charcoal and volatiles.

3. RESEARCH METHODOLOGY

3.1 Material

The material that was used in this study was Eucalyptus pellets that were provided by a local paper and pulp company, that were residues of their eucalyptus debarking process. The material was pelletized and sent to the CERENA laboratory in Lisbon to perform different tests. On table 3 the proximate and ultimate analysis was provided by the company.

Proximate analysis	
Parameter	Value
Moisture (%)	10,2
Volatile matter (dry %)	78,1
Fixed carbon (dry %)	17,5
Ash (dry %)	4,5

Ultimate analysis	
Parameter	Value
Carbon (%)	46,4
Hydrogen (%)	5,7
Nitrogen (%)	0,7
Sulfur (%)	nd
Oxygen (%)	42,3
Chlorine (%)	0,4
ash (%)	4,5

Table 3. Proximate and ultimate analysis of material.

The samples that were prepared for all the test were taken in the lab and the size was reduced from a pellet and grinded into powder that could be more easily fitted into the TGA/DSC equipment for a proper experimental procedure.

3.2 Equipment

The equipment that was used for the experiment was a TA Instruments SDT 2960 simultaneous DSC-TGA apparatus. This equipment has a furnace that can be used up to 1500°C, a couple of thermoelectric disks measuring heat flow, and a balance that records the weight of the sample during the experiment. On these disks, 2 pans will be placed, one will carry the material for the experiment, and the second will be a blank pan that will be used as reference. The equipment has connection to 3 gas feeding lines: a line that provides air, a line that provides nitrogen, and a line that provides CO₂. There is a digital flow meter that ensures that all the experiments were taken at the same flow (20 ml/min). The device is connected to a computer in which all the data is received and processed; giving as an output the data that was recorded (time, temperature, weight of sample, derivative weight, and heat flow). The system also delivers graphics of these curves for analysis.

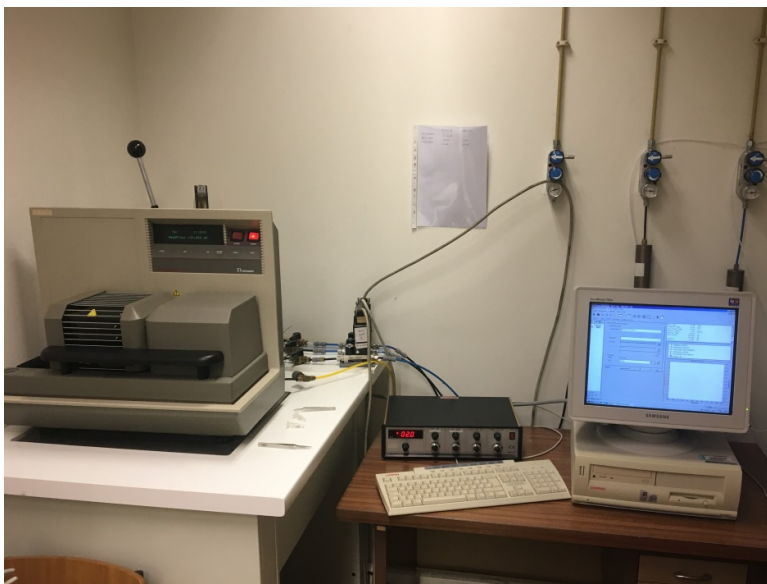


Figure 15. SDT 2960 simultaneous DSC-TGA equipment with computer.

3.3 Experimental method

All the experiments carried-out this study were carried-out using a simultaneous TG/DSC apparatus that allowed the simultaneous collection of TG and DSC data. In the data analysis section this work is divided into 2 parts: the first was a thermogravimetric analysis (TGA) and the second one is a differential scanning calorimetry (DSC) test. The material which is subject to a test is exposed to a controlled heating program in a controlled environment (highest temperature, gas flow, heating rate, type of heating gas). The TGA analysis provides information on profile of loss material and the rate in which the mass is lost. The DSC signal shows the heat data of the process, if it was released or if it was absorbed during the experiment, and the temperature in which the event occurred.

The experiment began with the selection of the gas that was going to be used for the test, and then, in the equipment balance, the 2 pans will be placed and then the equipment is tarred. After this, the pan that will carry the sample will be taken out and the sample will be put in (approximately 10 mg of sample), and it will be placed in the equipment to start the test. The tests were done using a gas flow rate of 20 ml/min for all experiments, and followed the same steps for all the different gases which were done in this study, the experimentation steps are the following:

- Heat furnace to 40°C.
- Wait 10 minutes for stabilization.
- Heat up from 40°C until 900°C at given heating rate.
- Isothermal at 900°C for 10 minutes.
- Cool off temperature to ambient temperature.

- Finish experiment.

The heating rates that were used for this study were 4: 10 °C/min, 20°C/min, 50°C/min and 100°C/min.

The experiments were carried out under oxidative and non-oxidative atmospheres, and also, with partial oxidation atmospheres, with mixtures of air and CO₂. The following atmospheres were used for the experiments:

- Nitrogen.
- Air
- CO₂
- 75% air- 25% CO₂
- 50% air- 50% CO₂
- 25% air- 75% CO₂

3.4 Data processing and calculations

The calculations for all the experiments were done in excel software, for analysis and also for calculations involving model fitting. The process of calculating the model to fit the data is the following:

3.4.1 Biomass degradation analysis

The experimental data that was obtained in the tests is uploaded in excel. For each carrier gas, a plot of all their heating rates was done, plotting normalized weight vs temperature. An analysis was done for each one of the experiments done with gases explaining how the behaviour of the biomass degradation was affected by the different carrier gases and by the different heating rates. The same analysis was done for derivative weights, along with biomass degradation and temperature in one graph. An analysis was done to verify how the different stages of derivative weight relate to the carrier gas and the heating rate.

3.4.2 Heating flow analysis

Heat flow analysis was done based on the data of the Differential Scanning Calorimetry (DSC) recorded by the system. For this analysis, a graph was done in which the heat flow is plotted against the temperature for each carrier gas. This graph includes all the heating rates for the specific gas that is being analysed, and the analysis of how the heating rate and the carrier gas affect the energy consumption or emission is done.

The TGA data is also placed in one graph against the DSC data in order to analyse how is the behaviour of the biomass degradation related to the heating behaviour of the biomass. The analysis was done at the heating rate of 10°C/min comparing all the carrier gases between them, first, between oxidizing and partial oxidizing environments, and then, between non-oxidizing environments. Also, a

specific heat of reaction analysis was done, in which the heat flow (mW) is divided by the derivative weight (mg/min), with this, and knowing the enthalpies of formation of different compounds, estimation can be done to know which the different compounds that are being formed.

3.4.3 Curve model fitting calculations

A mass fraction will be created for the model simulation. This mass fraction will be plotted against the temperature and it will be compared with the real mass fraction loss against temperature. In order to describe the biomass mass fraction loss, the pseudo-component approach will be used, in which several partial components that are created will characterize the biomass loss profile and give a provisional amount of component content in the biomass.

For this study, there is an assumption and is that all the pseudo-components will behave as a first order reaction. The kinetic behaviour of this model will describe the amount of material that is lost in a given time for each pseudo-component, and follows the following equation:

$$-\frac{dw_{n,m}}{dt} = k_n(T) * W_{n,m} * P_{O_2} \quad (17)$$

Where:

$-\frac{dw_{n,m}}{dt}$ = Derivative weight of pseudo component n at given time m.

$k_n(T)$ = Reaction rate constant of pseudo component n at given temperature T. Given by the Arrhenius equation (9). For this study, the reference temperature in the Arrhenius equation will be 500 K.

$W_{n,m}$ = Amount of biomass of pseudo-component n at given moment of time m. The Euler's method was used to solve the set of differential equations that were used.

P_{O_2} = Partial pressure of oxygen.

At the end of each time step m, all the weights are summed up to have a new modelled weight, as it is presented on equation (18):

$$W_{total,m} = \sum W_{n,m} \quad (18)$$

Where:

$W_{total,m}$ = Total weight of modelled biomass at the time m.

$\sum W_{n,m}$ = Sum of all pseudo-components n at given time m.

After the weight is calculated, the least-square method approach was used in order to make the model data fit the experimental data, and this is done by comparing the experimental data that was given in the software and the model data that was created. The main objective is to make the square of the difference between these 2 values using the following formula:

$$f(W)_m = (W_{experimental,m} - W_{total,m})^2 \quad (19)$$

Where:

$f(W)_m$ = squared error between subtraction of experimental data and model data at given time m.

$W_{experimental,m}$ = Weight of biomass experimental data at given time m.

A final error sum is done for all the time steps to get a final error comparing the experimental and the model data:

$$Error = \sum_{j=1}^N f(W) \quad (20)$$

Error = Total error of the difference between the experimental data and the model data during the complete test.

N = Number of time steps that were present on the experimental data provided by the software.

The total error was used in solver tool in excel, as the objective function and minimize the error as much as possible, changing the Activation energy (Ea), the pre-exponential factor (A), and the initial amount ($W_{n,0}$) of each pseudo-component, so the biomass degradation curve can fit the best with the experimental curve, and being able to make the best prediction for the biomass degradation for each one of the tests.

For this test, the main objective is to be able to model a single set of kinetic parameters (Ea and pre-exponential factor A), for all the heating rates (10, 20, 50 and 100 °C/min), with the only variation of the initial amount of each pseudo-component ($W_{n,0}$).

In this document, 2 ways to confirm the curve fitting were used:

- Confirming a low square residual value.
- Using the correlation coefficient (R^2).

The correlation coefficient shows how close the model data is to the experimental data. Shows the percentage of the response variable variation. The International Confederation for Thermal Analysis and Calorimetry (ICTAC) kinetics committee published recommendations [47] to collect experimental thermal analysis data for kinetic computations, based on studies made on TGA, DSC and DTA data. They recommend that for experiments by different heating rates, the correlation coefficient (R^2) the correlation coefficient had to be greater than 0.994 between the model data and the experimental data, in order for the model data to be reliable.

3.4.4 Thermal model fitting

For each pseudo-component, a heat composition was also created, so for each pseudo component on a given time and at a given temperature, there will be a heat generation. The heat equation is the following:

$$Q_{n,m} = -w_{n,m} * cp_{biomass} * \frac{\Delta T}{\Delta t} - dw_{n,m} * H_n \quad (21)$$

Where:

$Q_{n,m}$ = Derivative Heat flow of pseudo-component n at a given time m.

$w_{n,m}$ = Biomass weight of pseudo-component n at a given time m.

$cp_{biomass}$ = Specific heat of biomass.

$\frac{\Delta T}{\Delta t}$ = Delta temperature divided by delta time, given by software.

$dw_{n,m}$ = Derivative weight of pseudo-component n at a given time m.

H_n = Heat of reaction of pseudo-component n.

At the end of each time step m, all the heat components are summed up to have a new modelled heat formed at the time m, as presented on equation (22):

$$Q_{total,m} = \sum Q_{n,m} \quad (22)$$

Where:

$Q_{total,m}$ = Total heat of modelled biomass at a time m.

The least-square method was also used in this experiment in order to fit the model data to the experimental data, in which the difference of the experimental value of the data is subtracted to the model data, and it's squared, as it is in equation (23):

$$f(Q)_m = (Q_{experimental,m} - Q_{total,m})^2 \quad (23)$$

Where:

$f(Q)_m$ = Squared error between subtraction between experimental heat data and total heat data at a given time m.

$Q_{experimental,m}$ = Heat of biomass experimental data at a given time m.

At the end all the squared errors are summed up for all the time steps in the experiment, in order to get a consolidated error (24):

$$Error = \sum_{j=1}^N f(Q)_m \quad (24)$$

Where:

$Error$ = Total error between the experimental data and the model data during the complete test.

N = Number of time steps that were present on the experimental data provided by the software.

As with the weight data, the solver feature in excel was used to minimize the error between the experimental data and the model data, using the sum of the squares of the residuals as an objective

function. For this process, the biomass weight ($w_{n,m}$) and the derivative weight ($dw_{n,m}$) were taken from the data calculated at section 3.4.3, and the specific heat of the biomass ($cp_{biomass}$), and the heat of reaction of each pseudo-component (H_n) was changed in order to minimize the difference between the experimental and the model data, and get the best prediction of the heat data. The correlation coefficient (R^2) was also used as a quality measure to compare the compatibility between the experimental and the model data.

4. RESULTS AND DISCUSSION

After the experimental data was gathered, different types of analysis were done to the data, which are the following:

- TGA/ derivative weight curves analysis.
- Heat flow analysis.
- TG vs DSC analysis.
- Specific heat of reaction analysis.
- Kinetic model fitting.

4.1 TGA/ derivative weight curve analysis

The heating rate plays a very important role in the mass degradation and derivative weight loss profile, as the rate profile determines the slope of the biomass degradation curve.

Derivative weight loss can be separated into different stages in which the process can be determined according to the component that is being degraded. This does not mean that only this component is being degraded, as the other components can also be reacting, but according to the temperature, there is one dominant component that is reacting.

In figure 16, a typical DTG profile is shown, and this curve can be separated into 4 main reactions, which are the following:

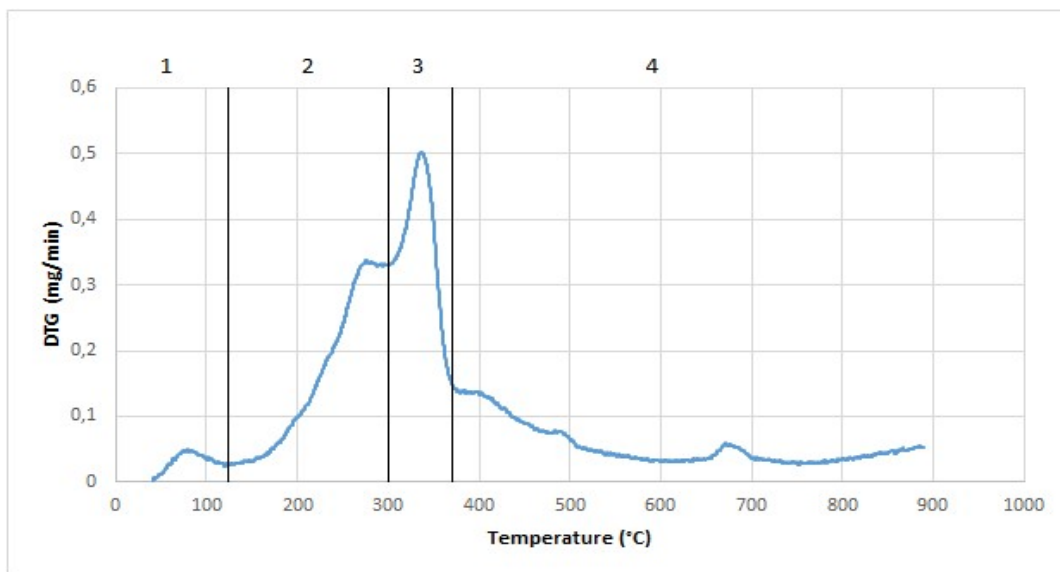


Figure 16. Derivative weight profile for pyrolysis test at 10°C/min heating rate.

Stage 1: Moisture loss. Amount of water in the biomass is evaporated in this stage.

Stage 2: Hemicellulose degradation. As the chemical composition of the hemicellulose is smaller compared to cellulose, it is the first component to degrade (see figure 3).

Stage 3: Cellulose degradation. Simple chemical structure makes a narrow temperature range to degrade most of the material, and it is shown mostly in a single peak, as shown in figure 2.

Stage 4: Lignin degradation. More complex chemical structure, as it has a wider variety of functional groups and bond strengths, makes the degradation of this structure more complicated. The final stage mainly degrades lignin structures until the end of the test.

The following analysis will check each one of the tests with air, CO₂, mixtures and the pyrolysis process. It will check the biomass degradation with the derivative weight, and compare each one of the degradation profiles, derivative weight loss and heating rates.

4.1.1 Pyrolysis

The pyrolysis test was done under the flow of nitrogen at 20 ml/min. The test was done under a constant ambient pressure, and a final temperature of 900 °C. Different heating rates were used as well, with 10°C/min, 20 °C/min, 50 °C/min, and 100 °C/min. figure 17 presents the results for the different heating rates

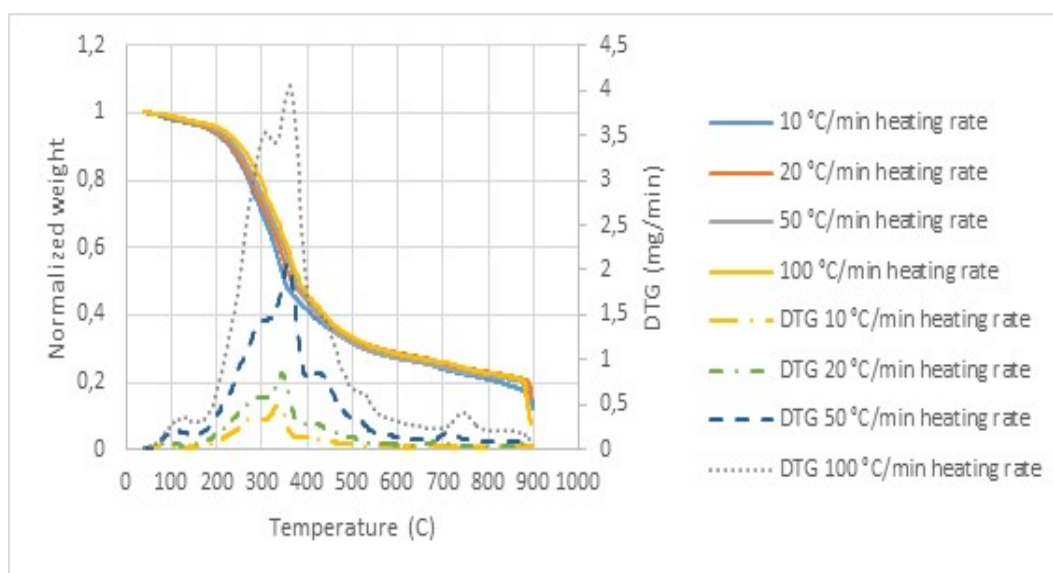


Figure 17. Biomass degradation profile and DTG curves pyrolysis at different heating rates.

The analysis of the pyrolysis curve degradation can be done in several stages:

First stage: Moisture loss, between 25- 140 °C. In this temperature a small amount of mass is lost, less than 10%, in which the moisture in the biomass is evaporated. Also, some light weight compounds are also released in this stage.

Second stage: This stage occurs in a range of temperatures between 200 °C and 320 °C, in which the hemicellulose and cellulose are decomposed[48]. Hemicellulose and cellulose reacts at lower temperatures compared to lignin. The largest mass degradation was seen in this stage, varying from 94% of mass to 55% of mass.

Third stage: In this stage, between 320° C and 450° C, the lignin is decomposed. In this stage, the mass degrades from 55% mass to 35% mass.

Final stage: In this stage, from 450 °C to 900° C, the residual lignin and residual char are decomposed. The residual lignin slowly decomposes on the temperature range, with a steady loss from 35% until the final weight of 10-15%.

The pyrolysis curve shows that the curve degradation is similar during the initial stages, and as the temperature increases, the behavior is different for each curve. The DTG curves shows a slow decreasing rate at the lowest heating rate, but as the heating rate increases, the DTG curve is having a higher degradation rate, until it has a very considerable degrading rate at 100°C /min. the degradation peaks are consistent at approximately the same temperature

All the heating rates have the same behavior, with a small change in the temperature. As the heating rate increase, the stages also increase. Table 4 has the information about the different stages and their percentage in which the highest mass degradation was found.

heating rate (°C/min)	1st stage temp (°C)	% mass	2nd stage temp (°C)	% mass2	3rd stage temp (°C)	% mass3	final temp (°C)	residual mass%
10	84,064	98,70%	275	78,60%	337	56,30%	900	14,10%
20	87,6	99%	287	76,90%	344,6	57,80%	900	15%
50	112,5	98,30%	295	77,07%	356,3	57,10%	900	13,60%
100	126,06	98,20%	306	76,80%	361	58,40%	900	8%

Table 4. Pyrolysis highest derivative weight peak and temperature vs heating rate.

4.1.2 Combustion 100% air

The combustion was done under the air, the tests were done at 20 ml/min and under constant atmospheric pressure and with a final temperature of 900 °C. Different heating rates were used, with

10 °C/min, 20 °C/min, 50 °C/min and 100 °C/min. Figure 18 shows the combustion results for the different heating rates.

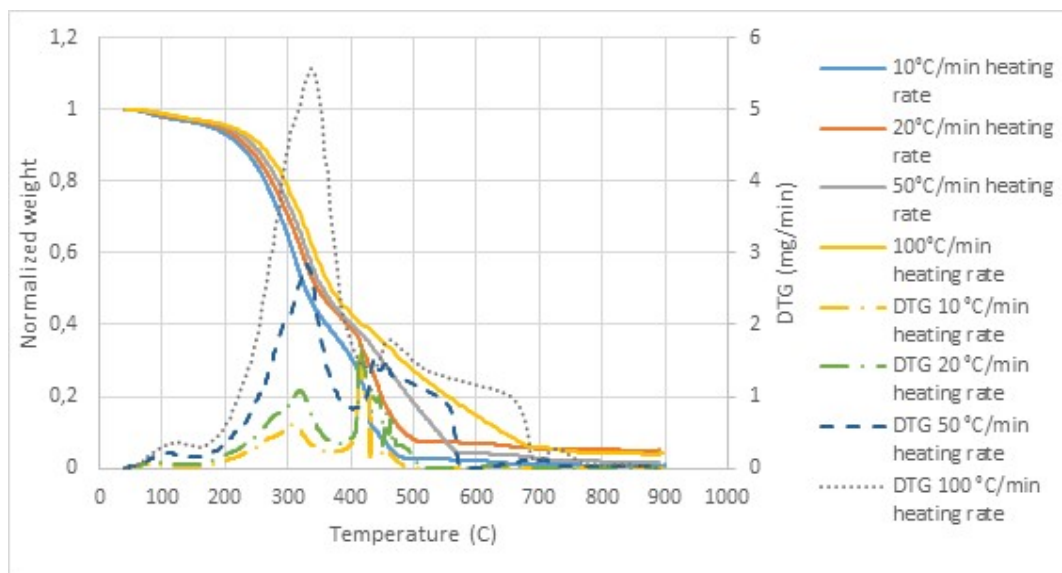


Figure 18. Biomass degradation profile and DTG curves combustion 100% air at different heating rates.

The analysis of the degradation profiles can be done in several stages:

First stage: Moisture loss, between 25- 140 °C. In this temperature a small amount of mass is lost, less than 10%, in which the moisture in the biomass is evaporated. Also, some light weight compounds are also released in this stage.

Second stage: Occurring between the temperatures of 150 °C and 350 °C. In this stage, the combustion process starts and degradation of biomass occurs from around 95% to approximately 40-45%. Also, cracking of complex components of the biomass into smaller compounds happen.

Third stage: Occurring between the temperature of 350 °C and 700 °C- The more complex compounds continue to crack and volatilize. Weight reduces from 40-45% to less than 8%, having a complete combustion. The ratio of weight degradation varies according to the heating rate. This is because the more complex compounds take more time to crack and need more time of exposure to high temperatures, changing the slope from the lowest heating rate to the highest heating rate.

The mass degradation curve is similar in the initial stages, but when the temperature increases, the mass degradation curves change and the values separate, having a much higher slope in the higher temperature rates. The DTG curves shows a big increase in the hemicellulose and cellulose degradation, beginning with a small degradation rate at a small heating rate, and increasing until it presents the highest decreasing rate at 100 °C /min, at around 340 °C. After this, the final combustion which was presented at 400 °C, in which at the lowest heating rates (10 and 20 °C /min), there is another increase in the DTG curve, until the material is finally degraded. For high heating rates, the DTG curves have an increase and a stable line following the mass degradation until the material is

completely degraded. Table 5 has the information about the different stages and their percentage in which the highest mass degradation was found:

heating rate (°C/min)	1st stage temp (°C)	% mass	2nd stage temp (°C)	% mass2	3rd stage temp (°C)	% mass3	final temp (°C)	residual mass%
10	73,43	99,20%	308,7	59,80%	426	25,70%	900	0,50%
20	86,3	99%	319,1	61,70%	416	34,20%	900	4,5%
50	111,8	98,30%	328	61,50%	436	33,30%	900	1,50%
100	121,9	98,10%	338,1	62,50%	461,1	33,60%	900	3,9%

Table 5. 100% combustion highest derivative weight peak and temperature vs heating rate.

4.1.3 Combustion 75% air-25% CO₂

The combustion was done under the flow of 75% air and 25% CO₂, the tests were done at 20 ml/min and under constant atmospheric pressure and with a final temperature of 900 °C. Different heating rates were used, with 10 °C/min, 20 °C/min, 50 °C/min and 100 °C/min. Figure 19 shows the combustion results for the different heating rates.

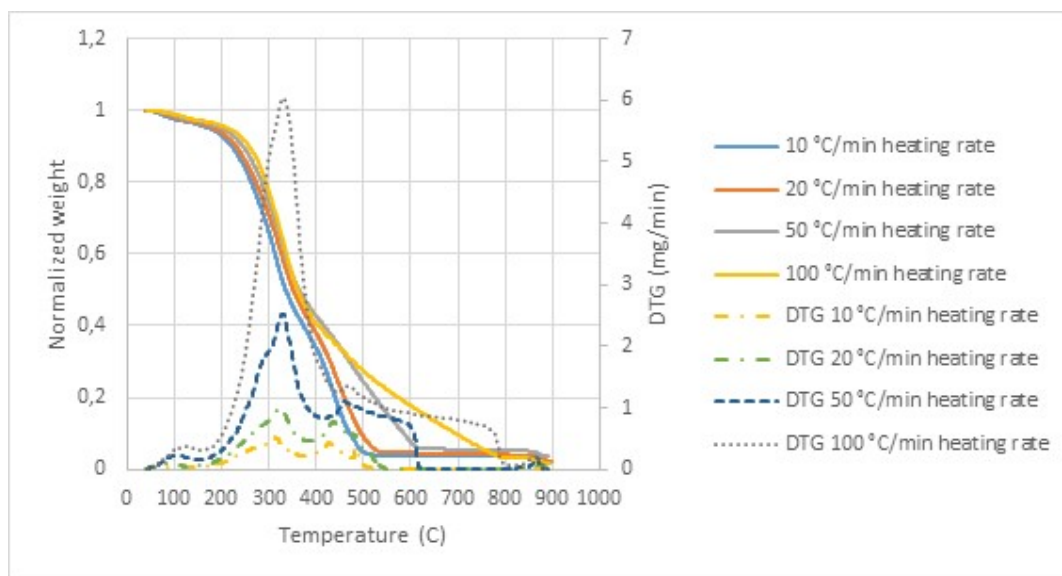


Figure 19. Biomass degradation profile and DTG curves combustion 75% air-25% CO₂ at different heating rates.

The analysis of the degradation profiles can be done in several stages:

First stage: Moisture loss, between 25- 140 °C. In this temperature a small amount of mass is lost, less than 10%, in which the moisture in the biomass is evaporated. Also, some light weight compounds are also released in this stage.

Second stage: Occurring between the temperatures of 150 °C and 350 °C. In this stage, the combustion process starts and degradation of biomass occurs from around 95% to approximately 40-45%. Also, cracking of complex components of the biomass into smaller compounds happen.

Third stage: Occurring between the temperature of 350 °C and 800 °C- The more complex compounds continue to crack and volatilize. Weight reduces from 40-45% to less than 5%, having a complete combustion. The ratio of weight degradation varies according to the heating rate. This is because the more complex compounds take more time to crack and need more time of exposure to high temperatures, changing the slope from the lowest heating rate to the highest heating rate. Also, in this stage, the influence of the CO₂ starts to be noticed, because the first 2 stages the behavior was very similar to the behavior on 100% air combustion. In this stage the slopes can be seen to be different having a higher temperature in which the biomass is finally degraded. When the test was being done under 100% air, at the heating rate of 10 °C/min, the temperature in which the biomass was degraded was around 450 °C. If this value is compared to the current test, the final temperature changes to 500 °C. The same happens to all the other heating rates, having a higher final temperature. This happens because the CO₂ acts like an inert gas at low temperatures (below 800 °C), so, the material degradation is slower. In this stage, there is a very small slope change at the end of the degradation zone, possibly happening because of the CO₂ influencing the gasification.

The behavior that is shown in the mixture of air-CO₂ makes the degradation and DTG curve to be similar to the 100% air scenario, the difference is that the temperature in which the biomass is completely degraded changes to a higher temperature, due to the fact that the CO₂ acts like an inert gas in low temperatures. The highest peak of material degradation is also seen at the temperature of hemicellulose-cellulose decomposition (about 340 °C), and also the highest degradation rate is seen at 100 °C/min heating rate. The trend is similar in the last stage of material degradation, as there is an increase in the DTG curve that maintains until the material is degraded. It is also noticed, that there is a very small peak at the DTG curves, occurring at almost 860 °C. This is because the influence of the CO₂ is starting to be present, as the gasification reactions are starting to appear in the residual mass that was not degraded. Table 6 has the information about the different stages and their percentage in which the highest mass degradation was found:

heating rate (°C/min)	1st stage temp (°C)	% mass	2nd stage temp (°C)	% mass2	3rd stage temp (°C)	% mass3	4th stage temp (°C)	% mass4	final temp (°C)	residual mass%
10	72,3	99,03%	310,1	61,40%	429,6	24,30%	483,6	7,40%	900	2,70%
20	92,7	98%	323	61,30%	438	27,20%	483	13,00%	900	2,2%
50	106	98,30%	328	62,90%	460,9	32,00%	-	-	900	3,80%
100	120	98,10%	330	63,90%	466,7	31,60%	-	-	900	1,5%

Table 6. 75% air- 25% CO₂ highest derivative weight peak and temperature vs heating rate.

4.1.4 Combustion 50% air-50% CO₂

The combustion was done under the flow of 50% air and 50% CO₂, the tests were done at 20 ml/min and under constant atmospheric pressure and with a final temperature of 900 °C. Different heating rates were used, with 10 °C/min, 20 °C/min, 50 °C/min and 100 °C/min. Figure 20 shows the combustion results for the different heating rates.

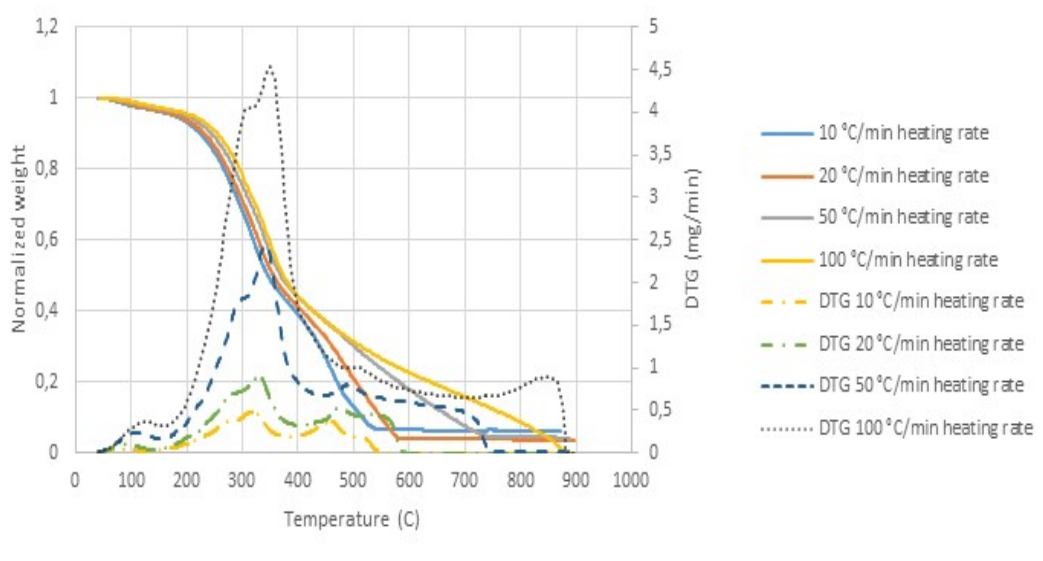


Figure 20. Biomass degradation profile and DTG curves combustion 50% air-50% CO₂ at different heating rates.

The analysis of the degradation profiles can be done in several stages:

First stage: Moisture loss, between 25- 140 °C. In this temperature a small amount of mass is lost, less than 10%, in which the moisture in the biomass is evaporated. Also, some light weight compounds are also released in this stage.

Second stage: Occurring between the temperatures of 150 °C and 370 °C. In this stage, the combustion process starts and degradation of biomass occurs from around 95% to approximately 40-45%. Also, cracking of complex components of the biomass into smaller compounds happen.

Third stage: The third stage is very similar to the one that was presented on the 75% air, 25% CO₂ scenario. The difference that can be seen is that, as there is more CO₂ present, the inert gas at lower temperatures is increased, and as a result, the final degradation temperature is higher than it was in the 75% air scenario. For example, at the lowest heating rate, of 10 °C, the temperature in which all the biomass is degraded is around 540 °C, compared to 500 °C, which was present on the 75% air scenario. Following the rest of the heating rates, it can be seen that all have a higher temperature as well, and with the 100 °C/min heating rate, the biomass degrades at approximately 870 °C.

As more CO₂ is getting into the mixture, it's influence on the rate in which the biomass is degraded can be seen, as now the temperature in which the biomass is degraded is higher compared to the

75% air scenario, due to the decrease in oxygen partial pressure, reducing the combustion rate. The maximum degradation ratio is following the same behavior than it did on the previous scenarios, having its maximum peak at approximately 340 °C, also, the highest degradation rate was observed at 100 °C/min heating rate. With this mixture, it was also observed that the highest heating rate, the final temperature of 900 °C was reached and it presented a small increase, occasioned by the CO₂ reactions that started to be manifesting, until the test was finished. . Table 7 has the information about the different stages and their percentage in which the highest mass degradation was found:

heating rate (°C/min)	1st stage temp (°C)	% mass	2nd stage temp (°C)	% mass2	3rd stage temp (°C)	% mass3	4th stage temp (°C)	% mass4	final temp (°C)	residual mass%
10	72,6	99,10%	317	61,03%	459	24,02%	510,2	11,03%	900	6,10%
20	89,3	98,6%	328	60,20%	472,5	27,50%	528	14,60%	900	3,7%
50	109,6	98,20%	341	60,10%	487,5	31,50%	-	-	900	3,90%
100	122,7	98,10%	350,8	58,90%	504,6	30,90%	-	-	900	0,0%

Table 7. 50% air- 50% CO₂ highest derivative weight peak and temperature vs heating rate.

4.1.5 Combustion 25% air-75% CO₂

The combustion was done under the flow of 25% air and 75% CO₂, the tests were done at 20 ml/min and under constant atmospheric pressure and with a final temperature of 900 °C. Different heating rates were used, with 10 °C/min, 20 °C/min, 50 °C/min and 100 °C/min. Figure 21 shows the combustion results for the different heating rates.

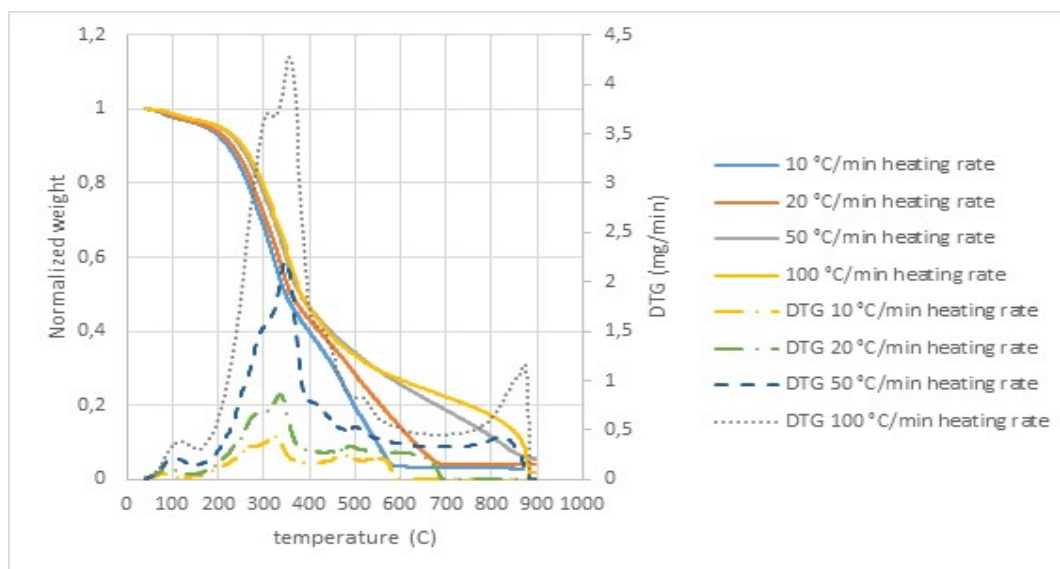


Figure 21. Biomass degradation profile and DTG curves combustion 25% air-75% CO₂ at different heating rates.

The analysis of the degradation profiles can be done in several stages:

First stage: Moisture loss, between 25- 140 °C. In this temperature a small amount of mass is lost, less than 10%, in which the moisture in the biomass is evaporated. Also, some light weight compounds are also released in this stage.

Second stage: Occurring between the temperatures of 150 °C and 400 °C. In this stage, the combustion process starts and degradation of biomass occurs from around 95% to approximately 40-45%. Also, cracking of complex components of the biomass into smaller compounds happen.

Third stage: In this stage, the effects of CO₂ are starting to be more visible, as first, the degradation is being more slow than it was on the 50% air scenario, in which now, the degradation curves start to have different slopes, with a higher temperature in which most of the biomass is degraded, for example, at the lowest heating rate, the temperature in which all the biomass is degraded is around 580 °C. On the higher heating rates scenario, as the biomass was not completely degraded before the final temperature, at around 800 °C, the CO₂ stops behaving as an inert gas and the gasification of this starts to react. As a result there is a small gasification reaction at the end of the test. On the highest heating rate (100 °C /min), the gasification was more evident, as the residual biomass was around 10% before the gasification process started, and after it could be seen how reacted at 850 °C.

There was a bigger influence of CO₂ in the reaction, as the slope of the material degrading is getting lower, indicating a slower process, due to the inert properties of CO₂ and the reduction of oxygen partial pressure. At the lowest heating rate (10 °C/min) the temperature in which the material is degraded is around 580-600 °C, compared to the previous scenario, in which the material was degraded at a lower temperature (500-520 °C). The highest peak of mass degradation was again found at the highest heating rate (100 °C), and at a temperature around 350 °C. At the highest heating rate (100 °C/min) the degradation of biomass was not complete at 800 °C, and as a result, there was a CO₂ gasification reaction taking place in the tests, as there was a fast degradation of material, and also having an increase in the DTG curve. Table 8 has the information about the different stages and their percentage in which the highest mass degradation was found:

heating rate (°C/min)	1st stage temp (°C)	% mass	2nd stage temp (°C)	% mass2	3rd stage temp (°C)	% mass3	gasification stage	% mass4	final temp (°C)	residual mass%
10	77,5	98,70%	319	60,00%	474	24,30%	-	-	900	2,70%
20	86,9	98,6%	329	61,30%	485	27,20%	-	-	900	2,2%
50	106	98,30%	342	62,90%	500	32,00%	867	4,50%	900	0,10%
100	117	98,10%	353	59,80%	515	32,60%	872	8,30%	900	1,8%

Table 8. 25% air- 75% CO₂ highest derivative weight peak and temperature vs heating rate.

4.1.6 100% CO₂ gasification

The gasification was done under CO₂, the tests were done at 20 ml/min and under constant atmospheric pressure and with a final temperature of 900 °C. Different heating rates were used, with 10 °C/min, 20 °C/min, 50 °C/min and 100 °C/min. Figure 22 shows the combustion results for the different heating rates.

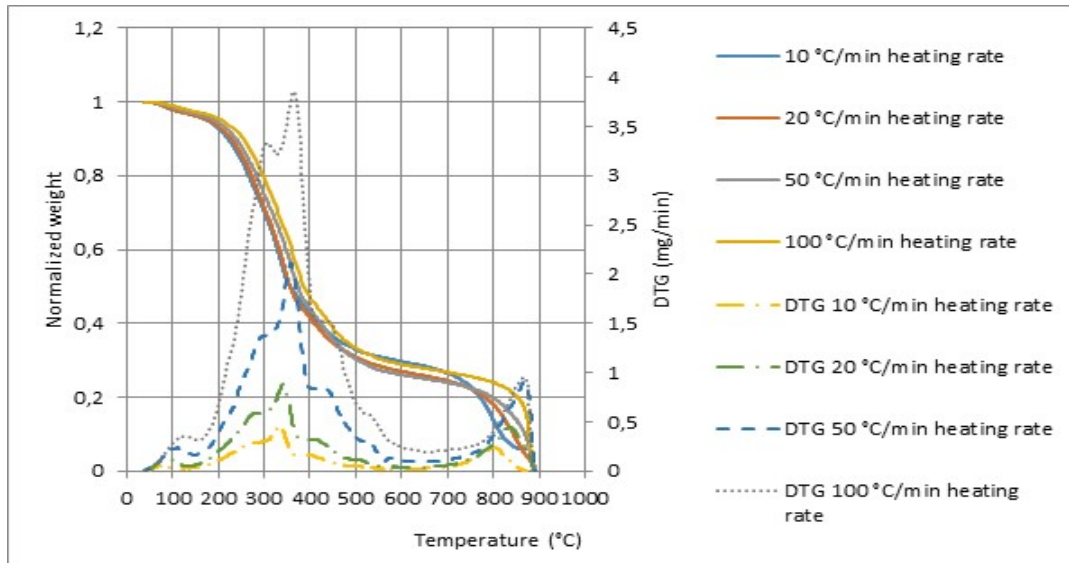


Figure 22. Biomass degradation profile and DTG curves Gasification 100 % CO₂ at different heating rates.

The analysis of the gasification can be done in several stages:

First stage: Moisture loss, between 25- 140 °C. In this temperature a small amount of mass is lost, less than 10%, in which the moisture in the biomass is evaporated. Also, some light weight compounds are also released in this stage.

Second stage: Occurring between the temperatures of 150 °C and 350 °C. In this stage, the combustion process starts and degradation of biomass occurs from around 95% to approximately 40-45%. Also, cracking of complex components of the biomass into smaller compounds happen.

Third stage: in this part, the temperature range changes from 350 °C up to 900 °C. In this stage, the first behavior is similar to pyrolysis degradation, as the biomass that is being degraded is lignin, similar to pyrolysis. CO₂ work as an inert gas at low temperatures and this is confirmed with the profiles presented. The material is being degraded until around 20% of the mass is left. The change is presented at around 750 °C, in which the gasification reactions start to be present. At this temperature, the material starts to degrade at a faster rate, as seen on figure 21. The heating rates changed the gasification speed, but mostly, the biomass was degraded at the end of the test.

The degradation rate changed, as now, the material is not completely degraded before reaching gasification temperatures, the material degrades until 400 °C, having the highest degradation peak at

350 °C, like in the other tests. On higher temperatures, it could be seen that the material degradation is done in a slow way, having a very constant slope on all heating rates, until it reached approximately 20% of material at 800 °C, and after this the CO₂ reactions take place, reducing the rest of the biomass, until it reached the final temperature of 900 °C. The DTG curves also show the degradation rate of the biomass at gasification temperatures, increasing between 800 and 850 °C. Table 9 has the information about the different stages and their percentage in which the highest mass degradation was found:

heating rate (°C/min)	1st stage temp (°C)	% mass	2nd stage temp (°C)	% mass2	3rd stage temp (°C)	% mass3	gasification stage	% mass4	final temp (°C)	residual mass%
10	84	98,50%	334,7	57,60%	497	33,20%	798,0	14,20%	900	5,80%
20	86,5	98,6%	345,6	56,60%	508	31,70%	838	12,20%	900	3,8%
50	110	98,10%	360	55,60%	525	30,10%	868	10,20%	900	0,10%
100	123,4	98,00%	369	55,50%	532	29,90%	868,5	15,70%	900	2,4%

Table 9. 100% CO₂ gasification highest derivative weight peak and temperature vs heating rate.

4.2 Heat flow analysis

Beside the mass degradation and the derivative weight, the heat flow was also recorded with the Differential Scanning Calorimetry (DSC) detector. This will allow showing the energy consumption property for the tests. Each test was recorder for all the different heating rates and for all the gasifying agents' tests.

4.2.1 Pyrolysis

Figure 23 shows the pyrolysis DSC curves at different heating rates: 10, 20, 50 and 100 °C/min:

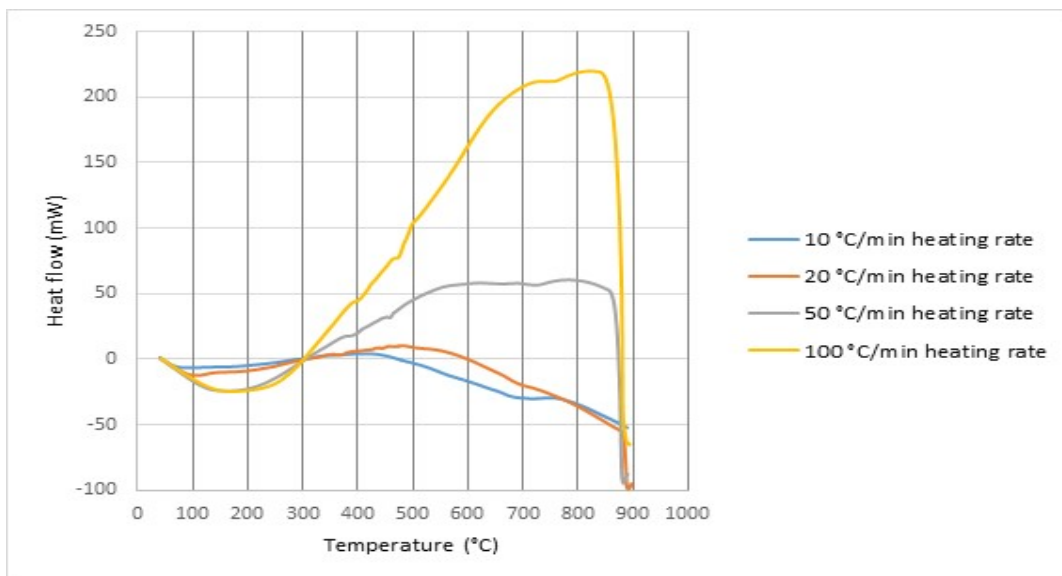


Figure 23. Heat flow DSC curves from Pyrolysis at different heating rates.

All the curves present the same behavior at low temperatures (below 120 °C/min) presenting an endothermic behavior, this is because the moisture that is present in the biomass is being removed. After this period, different behaviors are shown in the figure, one is presented at lower heating rates (10 and 20 °C/min), while another is present at high heating rates (50 and 100 °C/min), this is because at low heating rates, there is more time for the reaction to occur[48]. At low heating rates, there is an exothermic behavior between 120 °C and 500 °C. This is because hemicellulose and lignin reactions, and also different mechanisms at this temperature range are exothermic, presenting this behavior. At temperatures higher than 500 °C and up to 900 °C, there is an endothermic behavior, which is given because the DSC values for lignin, which dominates the degradation reactions at this temperature, have endothermic properties[48]. With higher rates, the behavior is different, as at higher reaction rates, the reactions presented an exothermic effect.

4.2.2 Combustion 100% air

Figure 24 shows the combustion with 100% air at different heating rates: 10, 20, 50 and 100 °C/min:

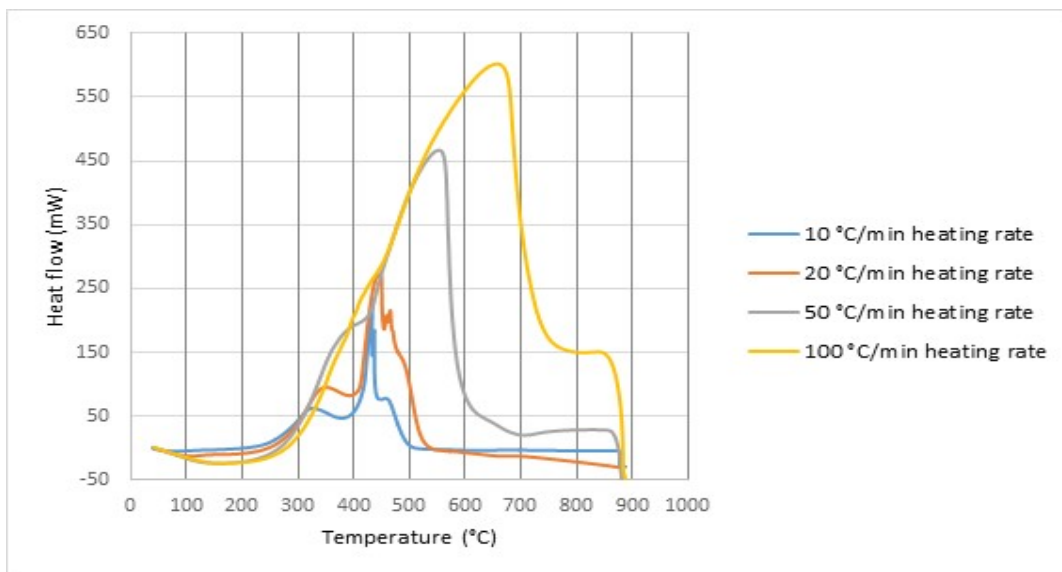


Figure 24. Heat flow DSC curves from Combustion 100% air at different heating rates.

Air combustion shows a similar trend in all the curves, and starts at lower temperatures, below 120 °C, in which the behavior of all the curves is endothermic, removing the moisture from the biomass. The second stage changes between the heating rates, but it is completely exothermic, and it is the combustion of the biomass, hemicellulose, cellulose and lignin. This operation occurs from 200 °C until 480°C for 10 °C /min, 500 °C for 20 °C/min, 600 °C/min for 50 °C/min, and 700 for 100 °C/min heating rate. The temperature changes because it is the time that takes the biomass to degrade completely, and the reactions to occur. There are 3 peaks that can be seen at low heating rates (10 and 20 °C/min) and this occurs because the first one is mainly the loss of volatile matter, while the second peak is due to the combustion of char. The third peak could be present because of lignin that was not degraded, as it has a wider temperature range compared to hemicellulose and cellulose. At high heating rates (50 and 100 °C/min) there is only one heating rate, which is done because of the fast increment of temperature, the reactions occur at the same time as the temperature is increasing. The amount of heat that is released on this process is the highest (approx. 600 mW for 100 °C/min) compared to the experiments mixed with mixtures of air- CO₂, this is because there is more oxygen in the gasifying agent, as there is only air, presenting a bigger release of heat.

4.2.3 Combustion 75% air- 25% CO₂

Figure 25 shows the combustion with 75% air- 25% CO₂ at different heating rates: 10, 20, 50 and 100 °C/min:

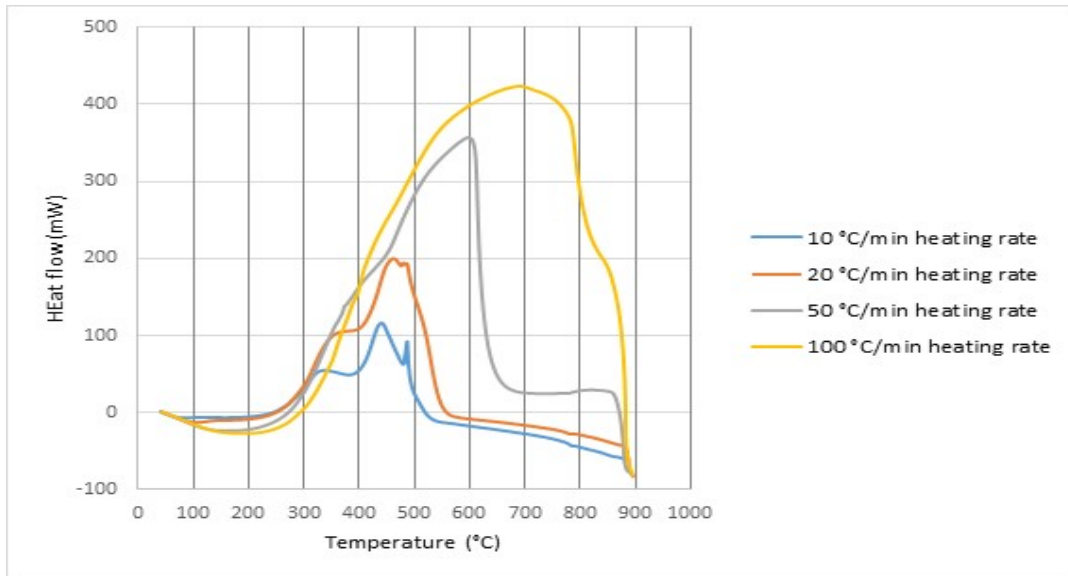


Figure 25. Heat flow DSC curves from combustion 75% air-25% CO₂ at different heating rates

This mixture of air and CO₂ has a behavior that is very similar to the 100% air test. The first part present endothermic characteristics up to temperatures of 120-130 °C. This is because the moisture is being removed from the sample. Then, an exothermic behavior is present, as the combustion of the biomass is taking place, with the difference that the maximum heat peak its being present at a higher temperature on the mixture temperature. This is because the CO₂ present in the mixture acts as an inert gas and slows the oxidation reactions of the biomass, having a higher temperature of reaction. For example, at 100 °C/min heating rate, it can be seen that the temperature in which the biomass is consumed is 700 °C, at the mixture; the biomass is consumed almost at 800 °C. Also, the heat flow is lower compared to 100% air. While at 100% air, and a 100 °C/min heating rate, the maximum heat flow is around 600 mW, with the mixture the maximum heat flow is over 400 mW, because of the lower presence of air in the mixture. The 3 peaks are still visible at lower heating rates, but with a smaller peak.

4.2.4 Combustion 50% air- 50% CO₂

Figure 26 shows the combustion with 50% air- 50% CO₂ at different heating rates: 10, 20, 50 and 100 °C/min:

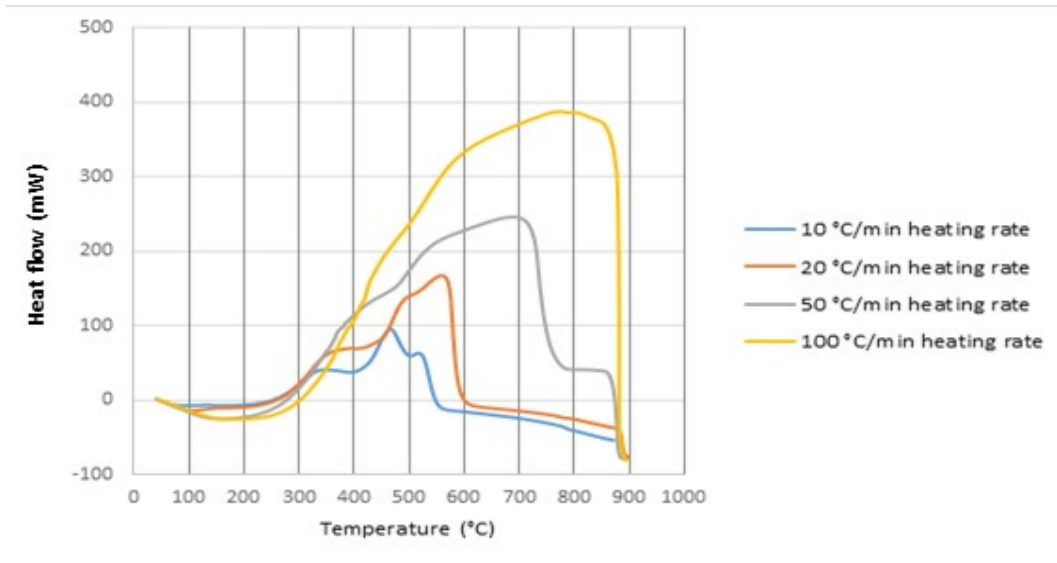


Figure 26. Heat flow DSC curves from combustion 50% air-50% CO₂ at different heating rates

The influence of CO₂ can be more visible in this test. At lower temperatures (lower than 120 °C) there is an endothermic behavior, due to moisture removal. At lower heating rates (especially at 10 °C/min), there is an exothermic behavior, due to the oxidation of the biomass, the 3 peaks are less visible this time. This phenomenon is also visible at 20 °C/min, but is not very clear. At high heating rates, the temperature in which the biomass reacts is higher than at the mixture of 75% air- 25% CO₂. This is because there is less air to react with the biomass and the CO₂ acts as an inert gas at low temperatures. The amount of heat released is also lower compared to the 75% air- 25% CO₂ mixture, also due to the lower amount of oxygen present in the gasifying agent.

4.2.5 Combustion 25% air- 75% CO₂

Figure 27 shows the combustion with 25% air- 75% CO₂ at different heating rates: 10, 20, 50 and 100 °C/min:

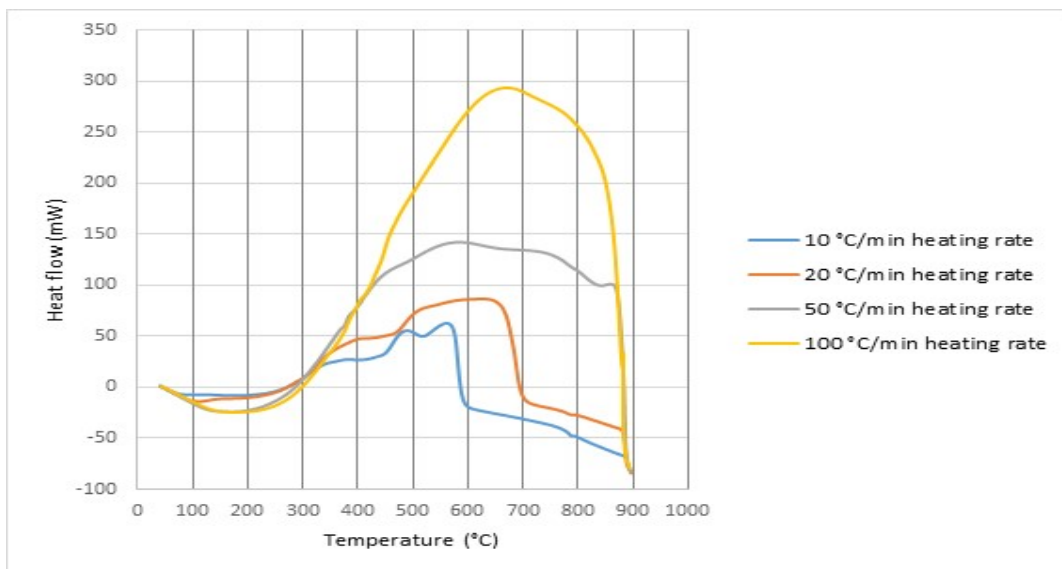


Figure 27. Heat flow DSC curves from combustion 25% air-75% CO₂ at different heating rates

The behavior on this mixture is almost the same at the beginning as it has been in the rest of the tests. At lower temperatures (below 120 °C) there is an endothermic behavior. At higher temperatures, the behavior is similar as the mixture of 50% air- 50% CO₂, as at low heating rates it could be seen 3 peaks, but with a very small peak height, also, the biomass was degraded at a higher temperature (600 °C at 10 °C/min, 700 °C at 20 °C/min), and, at a higher heating rates, the biomass is degraded almost at the end of the test, almost at 900 °C. The heat flow is also lower compared to the 50% air- 50% CO₂ mixture, as there is a smaller amount of oxygen present, making the CO₂ to influence the reaction mostly.

4.2.6 100% CO₂ gasification

Figure 28 shows the gasification of CO₂ at different heating rates: 10, 20, 50 and 100 °C/min:

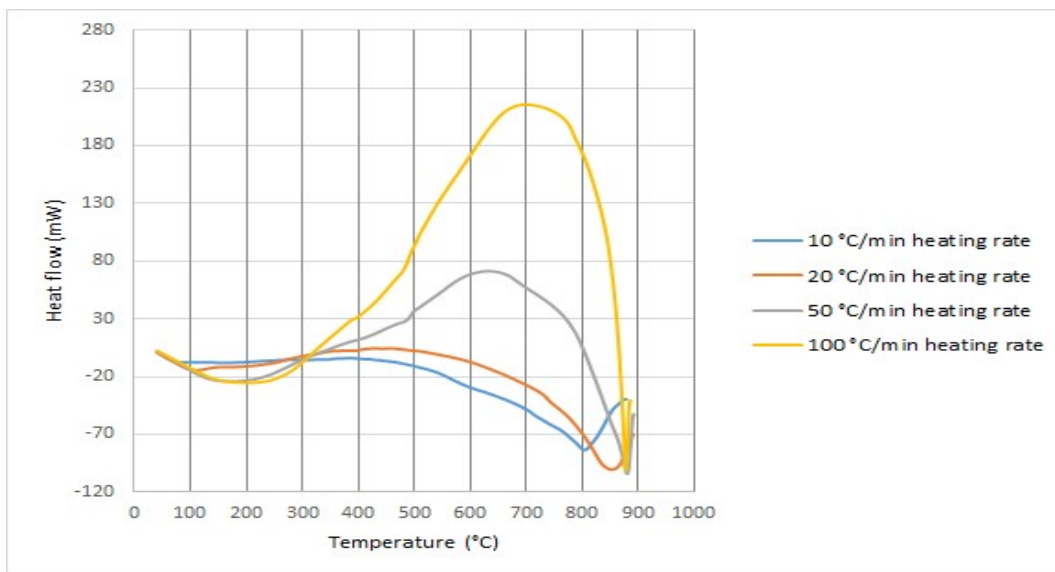


Figure 28. Gasification 100% CO₂ DSC curves at different heating rates

Without the effect of air and using 100 % CO₂ for the test a different response is found. At lower heating rates the heat response is almost endothermic all the time, being almost a constant endothermic profile close to 0 mW, up to 500 °C, and after that being completely endothermic with an increasing negative heat flow, this is because the lignin reactions after 500 °C are endothermic. This behavior continues to be similar until approx. 800 °C, temperature in which the behavior changes to have an exothermic trend. This is done because the CO₂ gasification reactions start to appear at this temperature. The char that was formed during the lower temperatures is gasified until it is degraded at the end of the test. At high heating rates, the behavior is very similar to the ones that appeared on the pyrolysis process, in which the reactions were exothermic until approximately 800 °C, but then decreased to be endothermic up to 850 °C, to finally start to appear the gasification reactions until the test was finished at 900 °C.

4.3 TG vs DSC curve analysis

Figure 29 shows the TG and the DSC curves for combustion of air, and partial combustion with 75% air, 50% air and 25% air/ CO₂ mixtures for a heating rate of 10 °C/min:

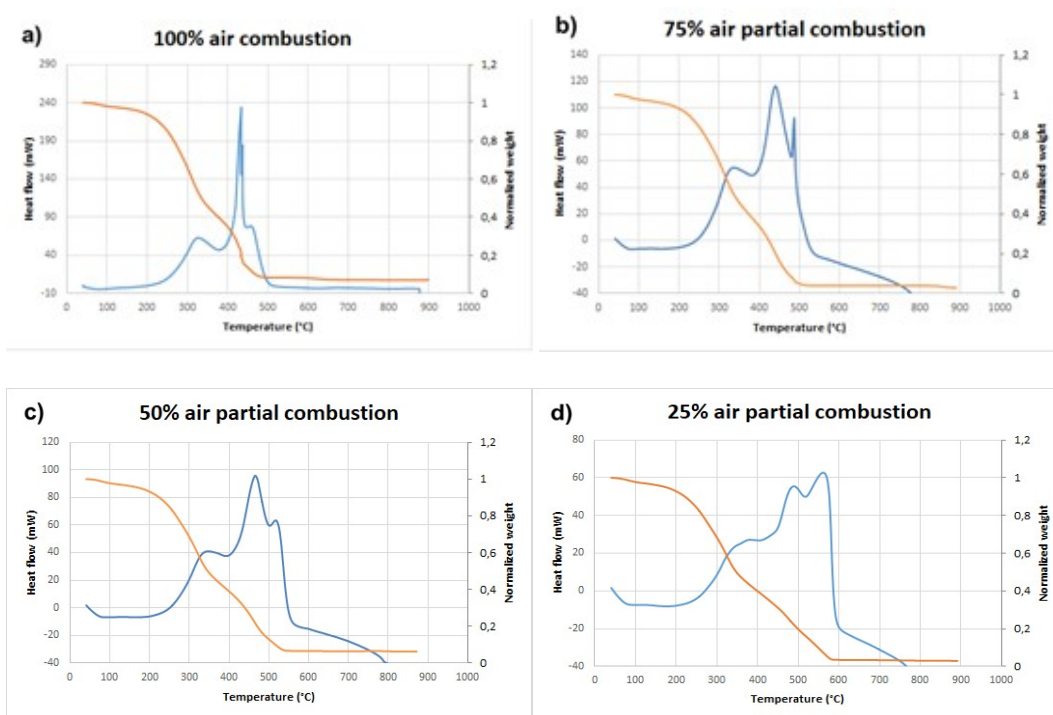


Figure 29. TG and DSC curves for 100% air combustion (a.), and partial combustion of 75% air (b.), 50% air (c.) and 25% air (d.) mixtures at a heating rate of 10 °C/min

The mass degradation curve added to the DSC curve can show some events that are being present on the reaction, and also, the effect of the CO₂ on the mixture of the gasifying agent. Firstly, it can be shown that there are 4 main events on all the tests, an endothermic section occurring at the beginning of the test, followed by 3 peaks that are occurring at the same moment that the mass is being reduced, as each peak reduce and the next one begin, there is a change in slope in the mass degradation curve, implying that there is another reaction taking place. As explained in section 4.2 the first peak represents loss of hemicellulose, the second cellulose degradation, the third lignin degradation and the fourth residual lignin and char reactions. Here it can be confirmed that 100% air combustion produces the highest amount of heat, with a highest peak of almost 230 mW, and as more CO₂ was introduced to the mixture, the highest power peak was being lower each time. This occurred because of the oxygen content of the gasifying agent. The highest peak was always found in the char combustion peak, except for the 25% air partial combustion, in which the highest peak was found in the residual lignin combustion. Also, the CO₂ is affecting the residual lignin combustion, as when there is 100% air combustion, there is only a small peak occurring, showing that almost all material reacted before. As more CO₂ was being introduced to the mixture, each time there was less air to perform the reactions, having a bigger amount of lignin at the end to combust, and presenting a wider peak as there was less air in the mixture. The heat that was generated on the lignin peak was varying between around 60 mW on the lowest amount of air (50% and 25%), to 90 mW on the highest amount of air (100% and 75%). Also, as there was more CO₂ on the mixtures, the reaction temperatures were higher, with the exception of volatile matter loss, which is almost similar in every test done.

Figure 30 shows the TG and the DSC curves for pyrolysis and CO₂ gasification for a heating rate of 10 °C/min:

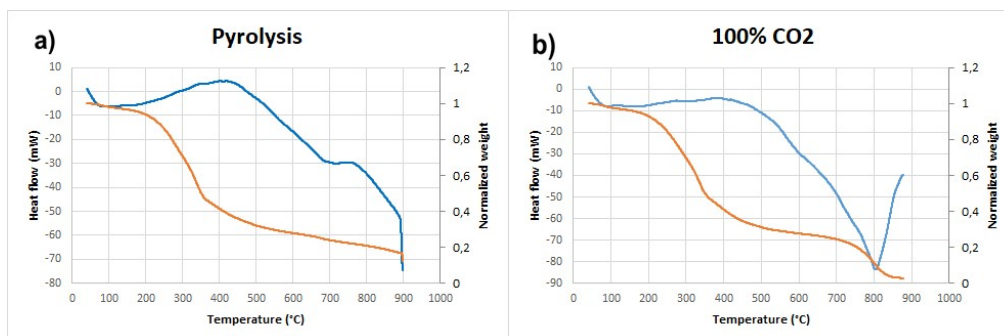


Figure 30. TG and DSC curves for pyrolysis (a.) and 100% CO₂ gasification (b.) at a heating rate of 10 °C/min

The mass degradation for pyrolysis and gasification with CO₂ has a similar behavior at lower temperatures, beginning with an endothermic section which is the moisture removal section. The next section that follows is from approximately 100 °C until 500 °C and is mostly exothermic, due to the different reactions and mechanisms in pyrolysis at this temperature. The charring process generated from hemicellulose is exothermic and it is presented in this stage. Both processes follow the same behavior. It can also be seen that the exothermic reactions finish at the moment that there is a change in slope on the mass degradation curve. At higher temperatures, the process becomes endothermic for both tests until 800 °C. Lignin reactions are endothermic at this temperature. At pyrolysis the process ends up with the endothermic trend reaching the final temperature, but with CO₂ gasification, there is an exothermic reaction occurring at approximately 800 °C, with a loss of mass happening at the same temperature range, until the test ends. This is because the CO₂ acts like an inert gas at lower temperatures, but at temperatures higher than 800 °C, the CO₂ reactions start to occur and the degradation of the mass was the char that was formed at lower temperatures.

4.4 Specific heat of reaction analysis

By dividing the heat flow by the derivative weight it can be calculated how much heat is being released or absorbed by each mg of biomass that reacted. With this information, and knowing the enthalpies of formation of the different compounds that are formed on biomass gasification reactions, which are mainly, CO, CO₂, H₂O, and CH₄, an estimation can be done of which compounds are being formed.

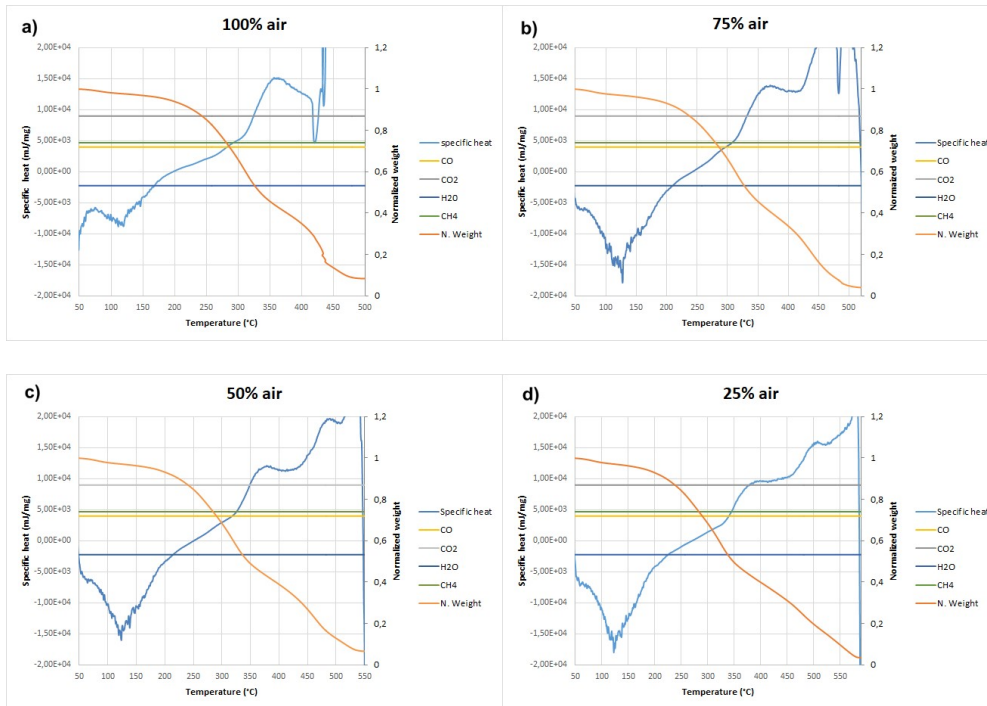


Figure 31. Specific heat of reaction curve for 100% air combustion (a.), and partial combustion of 75% air (b.), 50% air (c.) and 25% air (d.) mixtures at a heating rate of 10 °C/min with compounds heats of formation.

The specific heat can show a trend on the entire different tests that were done. At low temperatures (up to approximately 150 °C), there is an endothermic behavior on all of the tests, but at this temperature, the water that was contained in the biomass was being evaporated. After, there is an increase in energy having an exothermic behavior but now with small differences between each test. With 100% air, when the volatiles start to react (around 300 °C). When the volatiles start to react, the energy is above 5000 mJ/mg, indicating that there is now formation of CO and CH₄. The energy continues to increase with the volatiles combustion and the temperature increases as well, almost until 360 °C. The energy increases as well and the energy to form CO₂ is also reached. After this, there is a slow decrease until the char combustion is reached at over 400 °C and the energy increases until the biomass is consumed. For the different mixtures it can be seen that as more CO₂ is mixed in the gasifying agent, the temperature to reach the formation of the components is higher. It can also be seen that there is a smaller energy of reaction formed as more CO₂ is in the mixture. At 25% air-75% CO₂ it can be noticed that the energy of formation of CO₂ was barely reached, compared to the one presented on 100% air. This exercise allows to have a qualitative quick look at the components that are being formed, ratios can be calculated to get the amount of each component that is being formed. This is only an approximation, and could not be confirmed, as there was not an equipment available to measure the amount of gases that were formed.

4.5 Kinetic model fitting

The least square approach was used to fit a model to the experimental data, for all of the different heating rates and for all the different mixtures air-CO₂. The fitting of the models was evaluated with least squares approach and the correlation coefficient (R^2). This 2 quality checks allows verifying how close the modeled results are fitting the experiment data. On some experiments, there were only necessary to use 4 pseudo-components, but in others, 5 or 6 were necessary to fit the model. A global equation with global E_a and global k was developed to fit each heating rate, with the variation on the composition of the pseudo-components.

4.5.1 Combustion and partial combustion models

For combustion and partial combustion models, 4 pseudo components were used in order to characterize the biomass degradation profile, each component was intended to represent the 3 main components of lignocellulosic biomass (hemicellulose, cellulose and lignin), and also, the biomass moisture. The following figures represent some of the fittings that were done and their comparison to the experimental data that was gathered.

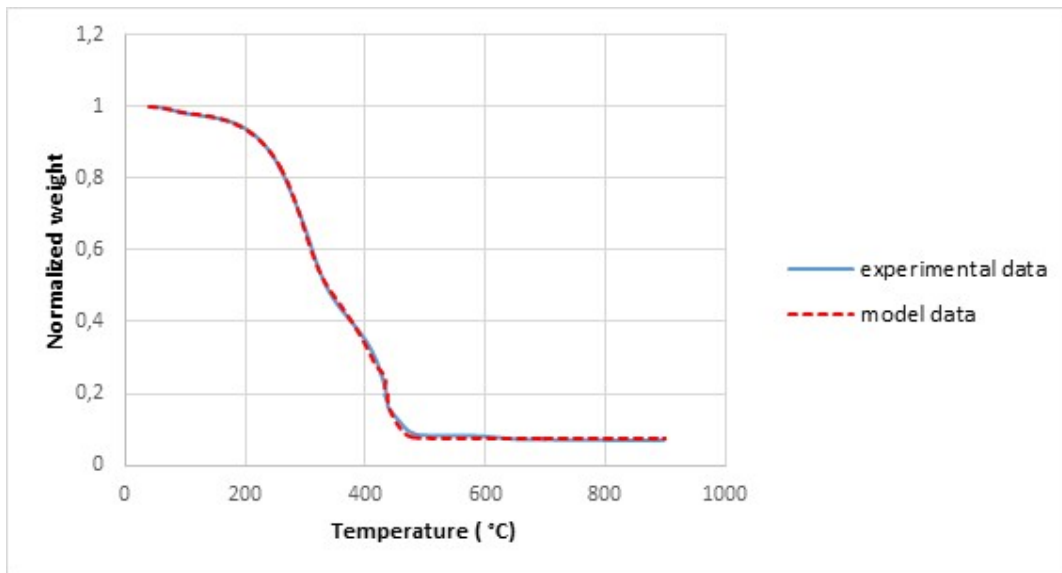


Figure 32. Biomass degradation profile of experimental and model information for air combustion at 10°C/min heating rate.

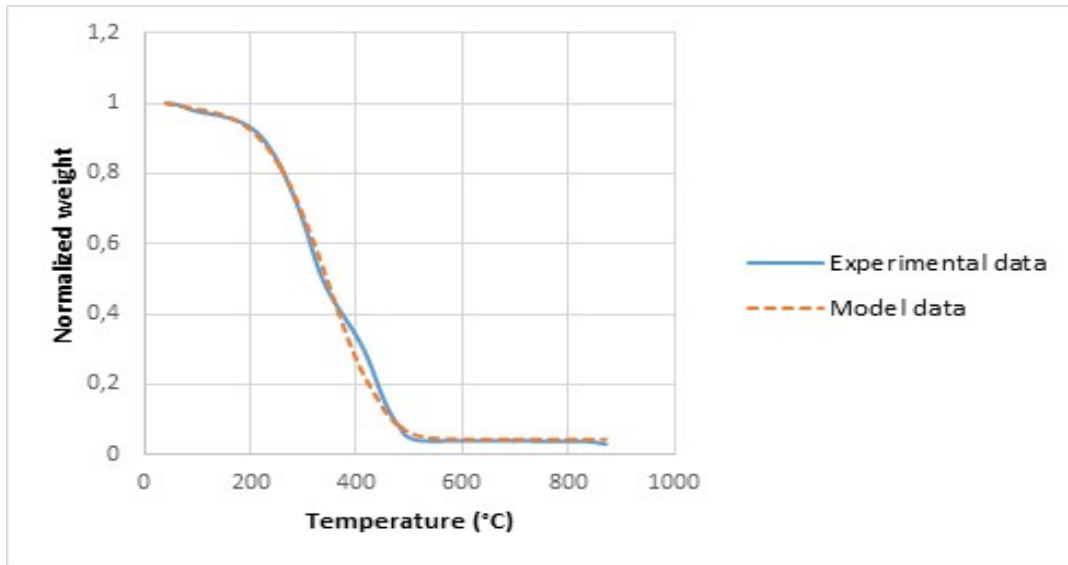


Figure 33. Biomass degradation profile of experimental and model information for 75% air- 25% CO₂ mixture at 10°C/min heating rate

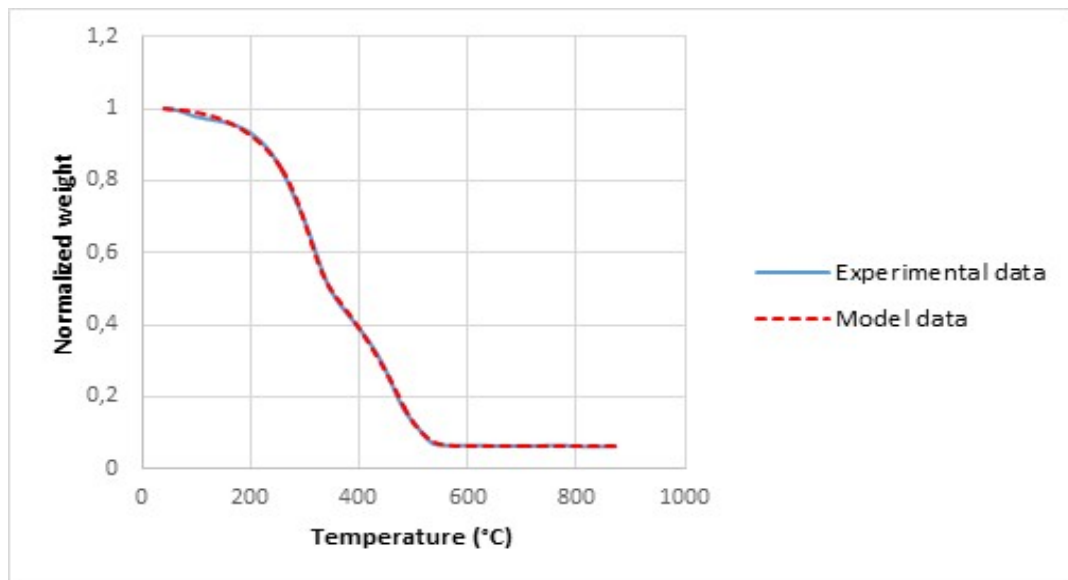


Figure 34. Biomass degradation profile of experimental and model information for 50% air- 50% CO₂ mixture at 10°C/min heating rate.

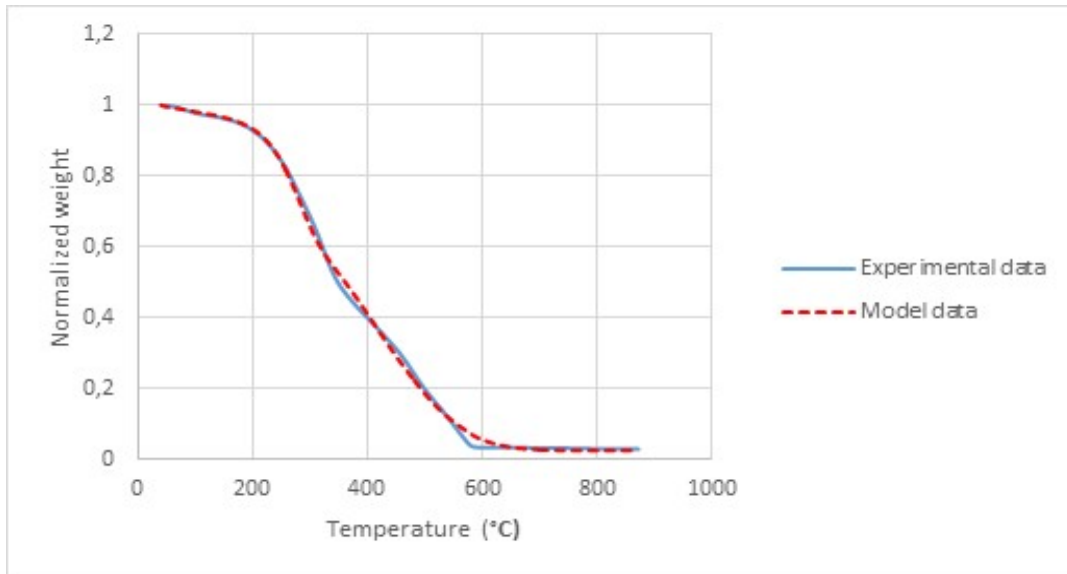


Figure 35. Biomass degradation profile of experimental and model information for 25% air- 75% CO₂ mixture at 10°C/min heating rate

As it could be seen on the figures, there is a good correlation between the experimental data and the model, as the curves are following each other, the red line is coinciding with the blue line, representing the experimental data. The kinetic parameters of the model (E_a and k) were fitted using the solver add-in in excel, calculating the least square method to minimize the error between the model data and the experimental data. A global set of kinetic parameters were done for each carrier gas, using one set to fit all the heating rates, changing the initial composition of each pseudo component, in order to fit the data.

The results of the kinetic parameters (E_a and k) are shown on table 10, for each one of the pseudo components that were used:

100% air				
	1	2	3	4
k (1/min)	11,51	0,22	0,000005	0,17
Ea (kJ/mol)	6,83	26,34	45,45	8,86
75% air- 25% CO2				
	1	2	3	4
k (1/min)	14,10	1,16	0,11	0,14
Ea (kJ/mol)	4,83	11,14	32,17	8,04
50% air- 50% CO2				
	1	2	3	4
k (1/min)	0,41	2,71	0,13	0,003
Ea (kJ/mol)	5,44	10,74	25,09	20,85
25% air- 75% CO2				
	1	2	3	4
k (1/min)	2,71	1,07	0,23	0,02
Ea (kJ/mol)	4,37	17,93	7,21	13,33

Table 10. Kinetic constants at reference temperature and activation energies for every pseudo component used in all of the oxidizing tests.

From table 10 different observations could be seen, that for the first pseudo component that characterize water evaporation, they all tend to have a similar activation energy (between 4.4 and 6.8 kJ/mol). The value of k was changing considerably from high amount of oxygen in the mixture to lower amount of oxygen, having a smaller value in the 50% air and 50% CO₂. The significant changes could be related to the small amount of water that is in the material compared to the other components, making any small change very sensitive to the model fitting. Figure 36 shows the rate constants and activation energies calculated for the component 1.

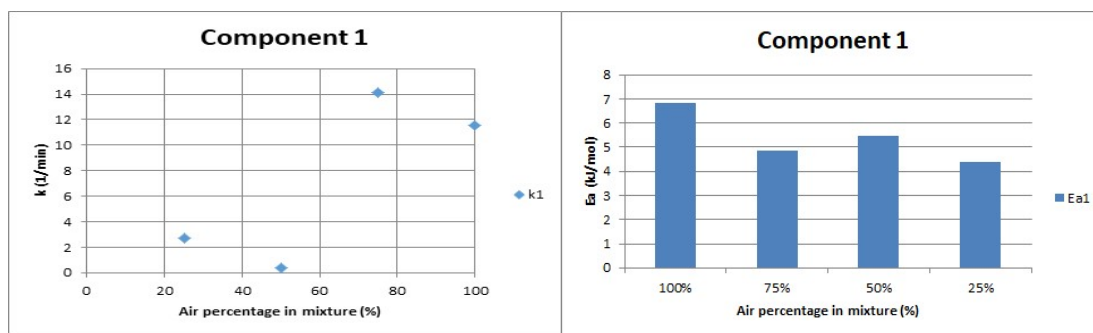


Figure 36. Constant rate and activation energy for component 1 at different mixtures of air and CO₂.

For the second pseudo component, it could be observed that this model had variations between the values of the components, and this was because this second pseudo component was having mixtures on their components, as sometimes characterized hemicellulose and lignin reactions, as it did on the

75% air- 25% CO₂ mixture, while other times only presented hemicellulose characterization like in the 50% air- 50% CO₂ mixture. It appears that apart from this behavior, there is no relation with partial oxygen pressure and the kinetics of the reaction, as it presented an independent behavior. Figure 37 shows the rate constants and activation energies calculated for the component 2.

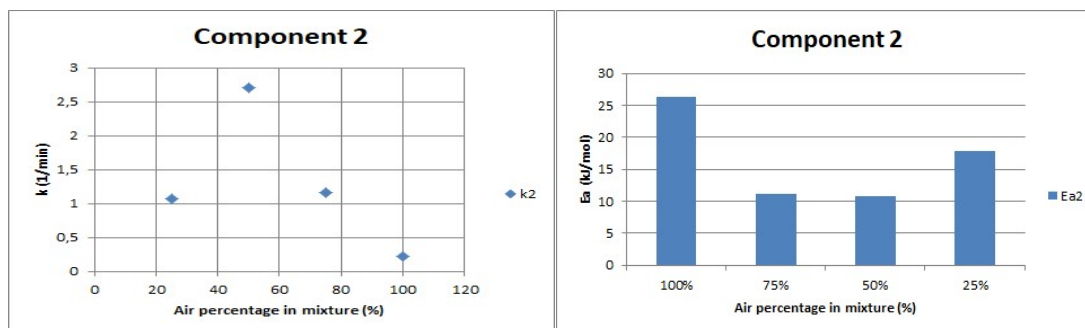


Figure 37. Constant rate and activation energy for component 2 at different mixtures of air and CO₂.

The third pseudo component, that was characterizing mostly the cellulose and char combustion, was showing higher activation energy with air as a gasification agent, but as more CO₂ was being introduced to the mixture, the activation energy was being lower. The behavior with the k factor was inverse, as the lowest value was reported for 100% air, and this value was increasing with the increment of CO₂ in the mixture. Figure 38 shows the rate constants and activation energies calculated for the component 3.

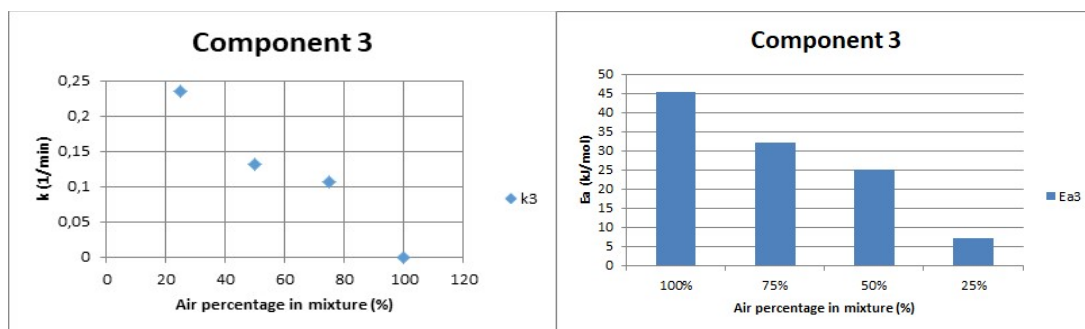


Figure 38. Constant rate and activation energy for component 3 at different mixtures of air and CO₂.

The fourth pseudo component was mainly characterizing lignin, which shows that there is a pattern that is stable at high partial pressures of oxygen, with an activation energy that is stable around 8 kJ/mol, but the activation energy increases with lower amounts of oxygen in the mixture. The biggest value was found at the 50% air- 50% CO₂, probably because on this mixture, the pseudo component

was also characterizing some residual char. Figure 39 shows the rate constants and activation energies calculated for the component 4.

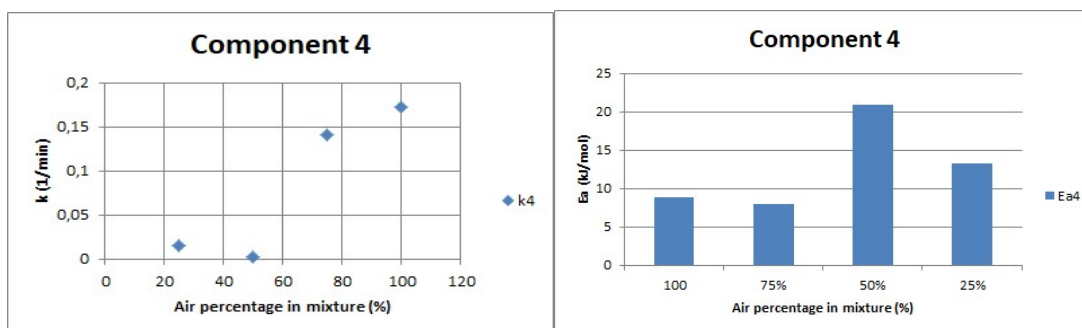


Figure 39. Constant rate and activation energy for component 4 at different mixtures of air and CO_2 .

To confirm that the models were having a good correlation with the experimental data, 2 sets of data were used, the residuals least square approach and also the correlation factor (R^2). Table 11 provides the information for the quality parameters.

Air- CO_2 ratio	10 °C/min heating rate		20 °C/min heating rate		50 °C/min heating rate		100 °C/min heating rate	
	Square error	R^2	Square error	R^2	Square error	R^2	Square error	R^2
100%	0,303	0,999	0,130	0,999	0,040	0,999	0,022	0,999
75%	0,986	0,998	0,323	0,998	0,225	0,997	0,044	0,999
50%	0,052	0,999	0,053	0,999	0,043	0,999	0,041	0,999
25%	0,504	0,998	0,195	0,999	0,202	0,998	1,324	0,991

Table 11. Model fitting quality parameters for all oxidizing tests. Square error residuals and correlation factor between experimental data and model data.

From the data it can be confirmed that all the models had a good correlation between the experimental data and the modeled data, as the correlation factors were all above 0.99, having a good quality and reliable data for the biomass degradation. The Square errors were small as well, which can say that the model data and the experimental data are very close to each other.

4.5.2 Pyrolysis model

For pyrolysis tests 5 pseudo components were used. A model was done for each of the heating rates using the least square method. Figure 40 shows the thermal degradation presented for the pyrolysis done at a heating rate of 10 °C/min.

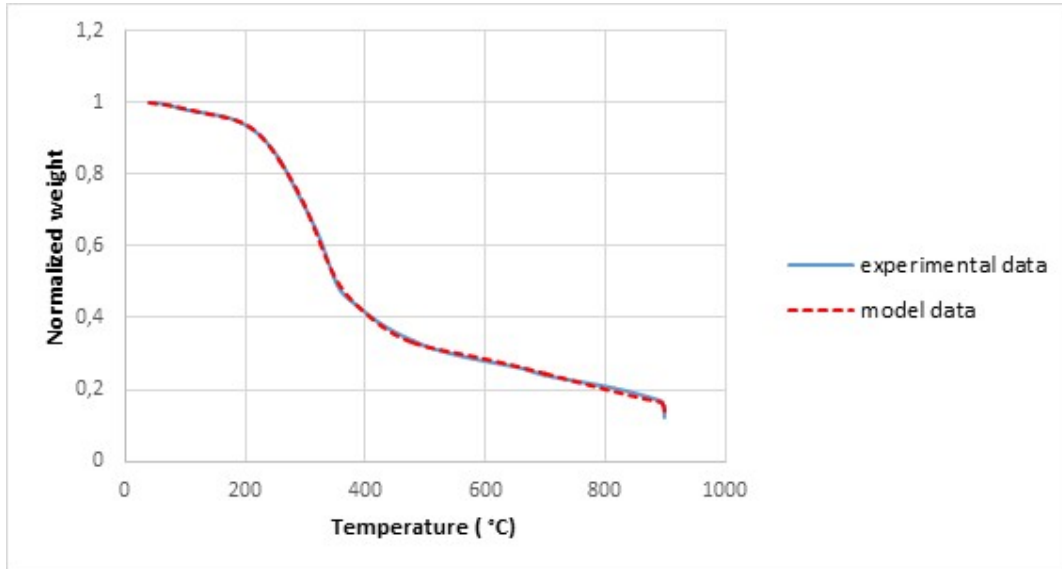


Figure 40. Biomass degradation profile of experimental and model information for pyrolysis at 10°C/min heating rate.

Table 12 shows the Ea and k for each one of the pseudo-components found for the model.

	1	2	3	4	5
k (1/min)	1,391	0,192	0,011	0,015	0,001
Ea (kJ/mol)	6,1312	18,8867	22,4299	9,8021	8,1221

Table 12. Pyrolysis model fitting parameters for all heating rates.

For pyrolysis was necessary to have 5 pseudo components, needing an extra one, because at high temperatures (above 600 °C) there is still being lignin material that is being degraded to char and this would not react as there is no oxygen to do the combustion, so, using 5 components (one for moisture, one for hemicellulose, one for cellulose, one for lignin, and one for residual lignin) gave the best results for the modelling.

The first pseudo-component has a behavior that is similar to the one that was found on the oxidizing tests, with an activation energy of about 6 kJ/mol, and a k value around 1 (1/min), which is similar to the numbers that were reported in the low oxygen content tests (low k value) having a consistent response.

The second pseudo-component which is correspondent to hemicellulose degradation, presents an activation energy of around 18 kJ/mol, which is also similar to the values that were reported for the mixture of 25% air-75% CO₂ (table 10) which had a value of 17 kJ/mol.

The third pseudo-component is the cellulose degradation component and has a value of around 22 kJ/mol. This showed a different behavior to the one that was presented on table 10, but it was found that this is because it is acting around the cellulose mostly, having a high amount of energy to release, compared to the oxidizing tests, in which lignin was appearing.

The fourth and fifth pseudo-element are mostly lignin degradation reactions, having smaller values of energy activation compared to hemicellulose or cellulose activation energies. Both activation energies have a very similar value (between 8 and 9 kJ/mol) confirming that in this stage, there is only lignin degradation reactions.

The models also had correlation comparison with the experimental data, and also the least square approach was done in order to verify that it was reliable. Table 13 shows the correlation and the square error of the model data compared to the experimental data:

	10 °C/min heating rate		20 °C/min heating rate		50 °C/min heating rate		100 °C/min heating rate	
	Square error	R2	Square error	R2	Square error	R2	Square error	R2
Pyrolysis	0,086	0,999	0,014	0,999	0,028	0,999	0,016	0,999

Table 13. Model fitting quality parameters for pyrolysis. Square error residuals and correlation factor between experimental data and model data.

All the data shows to have a very good correlation (more than 0.99) and a very small square error.

This confirms that the model is reliable and the data is good.

4.5.3 100% CO₂ gasification

The CO₂ gasification required of 6 pseudo components in order to be able to fit the model with the experimental data. Figure 41 shows the thermal degradation profile of the experimentation and the model that was used to fit the data. This figure shows the heating rate of 10 °C/min.

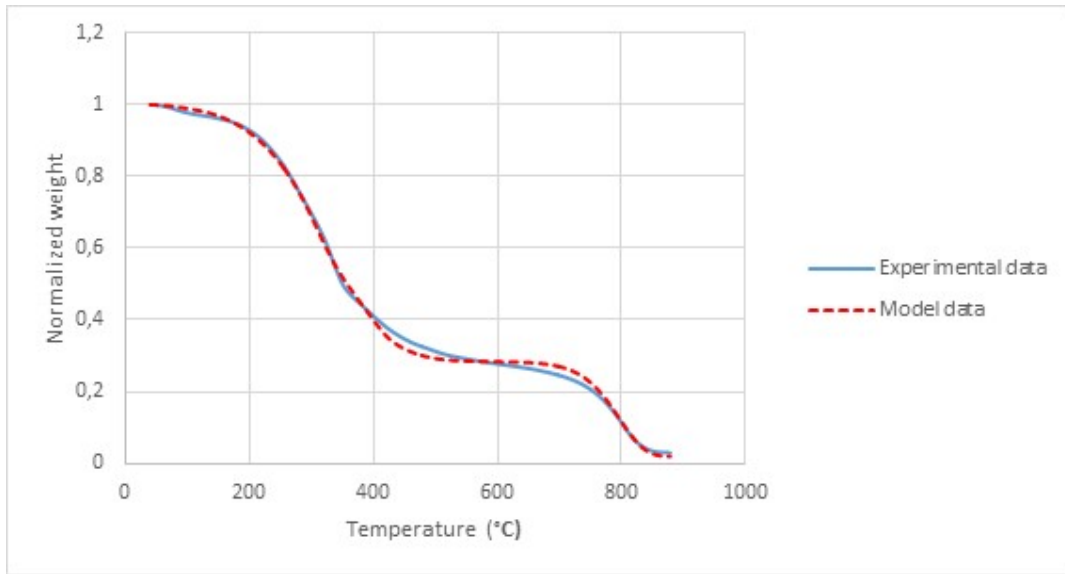


Figure 41. Biomass degradation profile of experimental and model information for CO₂ gasification at a 10°C/min heating rate.

Table 14 shows the values for Ea, and k of the pseudo components that were used for the model fitting.

	1	2	3	4	5	6
k (1/min)	67,63946	0,087065	5,08E-07	0,033965	0,011815	1,45E-14
Ea (kJ/mol)	12,9500106	16,9521348	55,3177654	6,62314347	25,2098043	60,668

Table 14. 100% CO₂ gasification model fitting parameters for all heating rates

The reason why it was necessary to use 6 pseudo-components is that the behavior of the CO₂ is similar to the behavior of the pyrolysis process, so 5 pseudo components were necessary to model the biomass degradation behavior, but with gasification, for temperatures higher than 800 °C, the CO₂ does not act like an inert gas, but starts to gasify the char that was formed, and this process was needed to be modeled as well.

The first component of modeling dealt with the moisture removal. The activation energy of this process was higher than the oxidation tests reported previously. This could be done because the kinetic of the reactions are different, as the carrier gas is different. This also has higher activation energy than the pyrolysis test.

The second pseudo component that is characterizing the hemicellulose degradation however, presents a similar trend to the values that were reported for pyrolysis test and the mixture of 25% air-75% CO₂ with an energy activation value of 17 kJ/mol.

The third pseudo component, that was characterizing cellulose degradation and in this occasion was a higher number than the ones that were presented previously. The kinetics of cellulose decomposition are more similar to the ones that presented the air combustion.

The fourth component described the lignin decomposition, giving values that were similar to the ones presented on the pyrolysis tests, with an activation energy of approximately 7 kJ/mol and a low k value (0.03 1/min). This behavior can explain that the lignin degradation follows similar kinetics on CO₂ and on pyrolysis.

The fifth pseudo-component has a larger value compared to the one that was presented on the pyrolysis test, probably due to the fact that this was residual lignin the values could be very sensitive as this could change depending on the amount of material that is on the experiment.

Finally the sixth pseudo-component is characterizing the char CO₂ gasification with a large activation energy value of around 60 kJ/mol and a very small k value.

The models also had correlation comparison with the experimental data, and also the least square approach was done in order to verify that it was reliable. Table 15 shows the correlation and the square error of the model data compared to the experimental data:

	10 °C/min heating rate		20 °C/min heating rate		50 °C/min heating rate		100 °C/min heating rate	
	Square error	R2	Square error	R2	Square error	R2	Square error	R2
CO2 gasification	0,688	0,998	0,207	0,998	0,323	0,998	0,145	0,997

Table 15. Model fitting quality parameters for pyrolysis. Square error residuals and correlation factor between experimental data and model data.

The correlation between the curves is less good that compared to the other mixtures with air, as the CO₂ reactions make the biomass degradation to have a different profile compared to air and mixtures. The model data is still valid, as the correlation factor is above 0.99, but compared to the other mixtures, the correlation is lower. The least square residual values are low, making also a good correlation between the model data and the experimental data.

4.6 Heat flow model fitting

A model to characterize the heating rate behavior was also developed in order to describe the characteristics of the biomass heat flow at the different gases and at different heating rates for each gas. The least squares approximation was also used to do this test. The correlation coefficient (R^2) was also used to evaluate the correlation between the experimental data and the simulated data. These models also were calculated using the same amount of pseudo-components that were used previously. So, for all the oxidizing tests, 4 pseudo-components were used, while that for pyrolysis, 5 components were used, and for CO_2 gasification, 6 components were used. In this section, the tests for air combustion, the mixture of 75% air-25% CO_2 and the pyrolysis tests will be shown and explained, the rest of the results will be shown in annex 1.

4.6.1 Oxidizing tests

For the oxidizing tests, 4 pseudo components were used, to characterize the 3 main components of lignocellulosic biomass (hemicellulose, cellulose and lignin), and moisture. The following figures show some figures of the experimental data and their comparison to the data that was modelled.

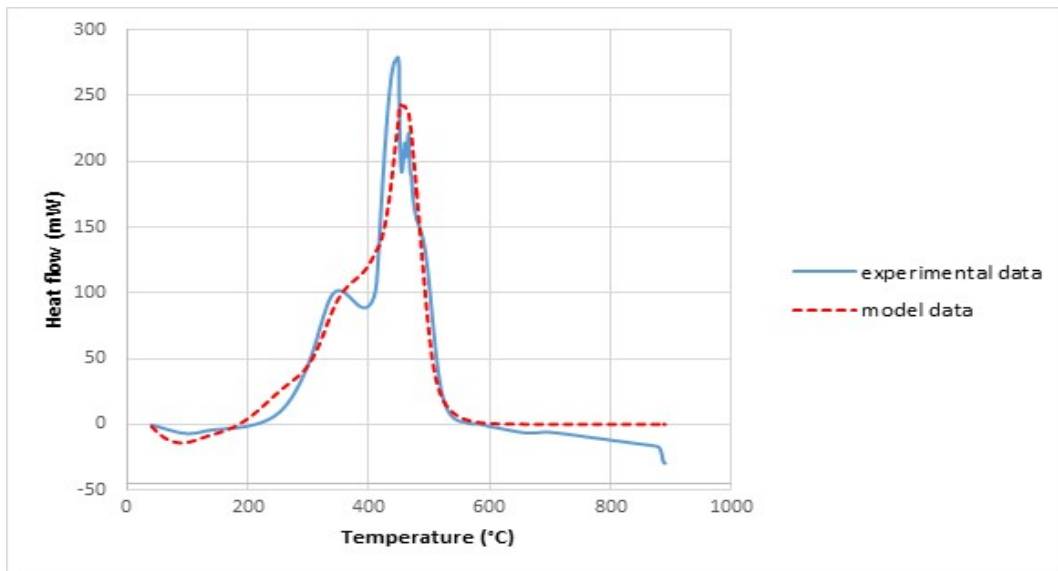


Figure 42. Heat flow experimental and model data for 100 % air combustion at a heating rate of 20 °C/min

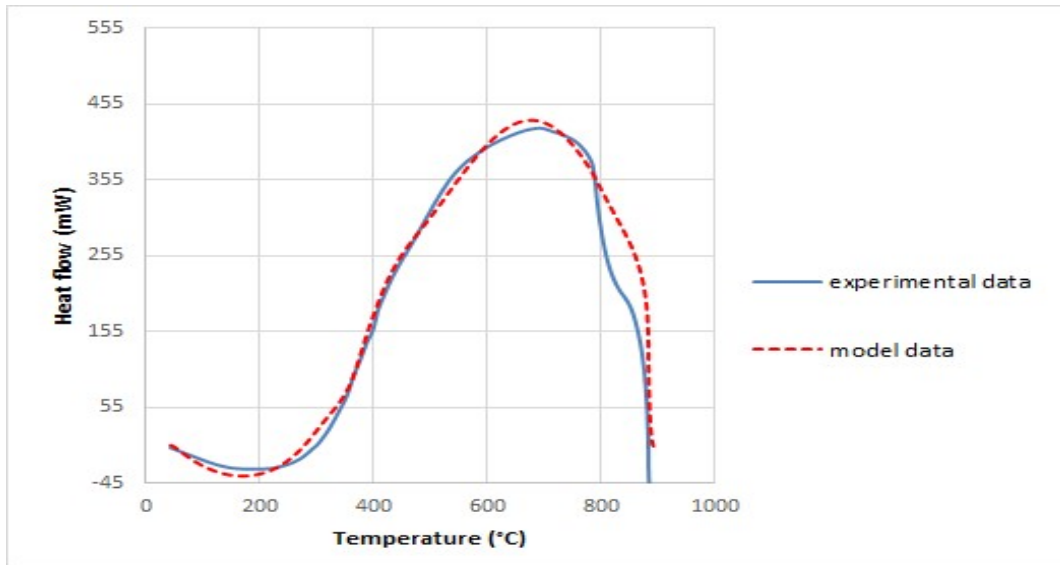


Figure 43. Heat flow experimental and model data for 75%air-25% CO₂ mixture combustion at a heating rate of 50 °C/min

The fitting of the models for the heat flow were more complicated to do, as the models were not having a good correlation between the experimental data and them. Table 16 and 17 will show the results of the modelling and the correlation of the experimental data and the models for air and the mixture of 75% air and 25% CO₂.

	Air combustion	1	2	3	4	R2
10 °C/min	Heat of reaction (kJ/g)	-510,641	134,393	-195,874	-107,170	0,889
	Cp (J/K)	0,076	0,076	0,076	0,076	
20 °C/min	Heat of reaction (kJ/g)	-0,006	21,646	-241,902	-116,482	0,924
	Cp (J/K)	0,047	0,047	0,047	0,047	
50 °C/min	Heat of reaction (kJ/g)	-136,719	-23,634	-293343	-130,803	0,96
	Cp (J/K)	0,077	0,077	0,077	0,077	
100 °C/min	Heat of reaction (kJ/g)	-111,722	-1,173	25,266	-238,521	0,963
	Cp (J/K)	0,068	0,068	0,068	0,068	

Table 16. Air combustion heats of reaction model parameters for all heating rates with correlation factor.

What can be observed is that the model used for fitting does not give a good correlation on low heating rates, as it can be seen on the table, the correlation factor was the lowest at the smallest heating rate (10 °C/min), while at 20 °C/min the behavior was still having a small correlation. The correlation factor at high heating rates was better (around 0.96), while it's not the best expected, it is better compared to the scenario at lower heating rates. This is because at low heating rates each component has the time to degrade and its own heat of reaction is being recorded, while at high

heating rates there are mixing reactions between each component, making a homogeneous reaction that is easier to characterize. This trend was seen on all the different tests that were done. For all the tests, it was decided to use one general C_p for each heating rate, this is why the results present the same C_p in one test. It can be observed that for the first pseudo component, there is always a negative value of heat of reaction, given because this component is representing the water evaporation, which is an endothermic process.

75% air- 25% CO ₂		1	2	3	4	R2
10 °C/min	Heat of reaction (kJ/g)	-313,421	1,007	640,123	-138,001	0,72
	C _p (J/K)	0,161	0,161	0,161	0,161	
20 °C/min	Heat of reaction (kJ/g)	-108,795	139,217	-2,002	-179,026	0,912
	C _p (J/K)	0,067	0,067	0,067	0,067	
50 °C/min	Heat of reaction (kJ/g)	-250,461	-19,453	-138,634	-448,657	0,975
	C _p (J/K)	0,107	0,107	0,107	0,107	
100 °C/min	Heat of reaction (kJ/g)	-148,048	-95,964	25,279	-334,720	0,989
	C _p (J/K)	0,097	0,097	0,097	0,097	

Table 17. 75%Air-25% CO₂ combustion heats of reaction model parameters for all heating rates with correlation factor.

Table 17 confirms that the models are difficult to fit the experimental data with low heating rate tests, but it improves on high heating rates. The first pseudo-component describes the water evaporation with a negative heat of reaction. At 50 °C/min the reactions that are occurring would appear to be all negative, that could be done because all the reactions from the biomass are being mixed giving a homogeneous response as it was seen on figure 48. The same behavior was present on 100 °C/min heating rate.

5. CONCLUSIONS AND RECOMMENDATIONS

5.1 Conclusions

This section will cover a brief summary of all the relevant aspects that were found during the development of this thesis, including the objectives and the result that were revealed.

The objective of the thesis was to perform a kinetic study to a specific type of biomass which is common in Portugal (Eucalyptus) and it is a residue of the debarking process. This study included different oxidative environments (air), non-oxidative environments (nitrogen and CO₂), and different mixtures of air- CO₂ (25%air-75% CO₂, 50%air- 50% CO₂, 75%air-25% CO₂) at different heating rates (10, 20, 50 and 100 °C/min).

Firstly, the biomass degradation and derivative weight profile were checked for every carrier gas test and all the heating rates. For biomass degradation profile, it was found that for pyrolysis the heating rate presented a similar behaviour, the difference was that at a higher heating rate the volatiles were degrading at a higher temperature, and the char was not completely degraded. At the end of the test, char was still present on the residual weight (approx. 10-15% of the weight in all of the tests). For air combustion, there was no difference between all the heating rates, except for the lignin degradation, in which at higher heating rates, the degradation was done at higher temperatures. As CO₂ was started to be mixed with air, it could be seen that the degradation temperature was higher than with air, due to the influence of CO₂ in the mixture, which acts like an inert gas. As more CO₂ was mixed, the degradation temperatures were higher as well. When CO₂ was used, the behaviour of the degradation profile was similar to the pyrolysis curves, until the gasification temperatures were reached, in which the gasification reactions took place, degrading the char that was formed at lower temperatures. For the derivative weight analysis the following highlights were found. For pyrolysis, the highest heating rate was presented at the cellulose degradation stage. For combustion, it was seen that for high heating rates (50-100 °C/min), the lignin was degraded at low temperatures (below 500 °C), while they require higher temperatures to degrade at high heating rates. (Around 700 °C). When CO₂ was added to the mixture it was seen that it was required to have more temperature to degrade the biomass. At 50%-50% mixture of air and CO₂ it could be seen that at high heating rates there were gasification reactions as after 800°C there was a peak in the derivative weight curve. With CO₂ for all heating rates not all the biomass is degraded, as there was a char forming at low temperatures, but after 800°C, the char that was formed was consumed, as at these temperatures there were CO₂ gasification reactions taking place. All the behaviours that were explained before, can confirm that the heating rate plays an important role in the degradation profile of the biomass, as the higher the heating rate, the higher the degradation temperature of the complex structures was. Also, it could be seen how the derivative weight was higher as the heating rate was higher, especially for degradation of simple structures (hemicellulose and cellulose). CO₂ also plays an important role in affecting the degradation temperatures of the biomass. As more CO₂ was being introduced into the atmosphere, the degradation temperatures were higher for the biomass sample. This is because of the inert gas properties that the

CO₂ has at low temperatures (below 700 °C), and because there is less oxygen that was replaced by the CO₂ in the mixture. It was confirmed that CO₂ starts to behave as a gasifier agent at high temperatures (above 700°C), when the 100% CO₂ test was done, the residual char that was formed was gasified at temperatures above 700°C.

A heating rate analysis was also done for all the carrier gases and all the heating rates. For pyrolysis tests, it was found that the behaviour was different at low and high heating rates. At higher temperatures (above 500 °c) the higher heating rates, it presented an exothermic behaviour, while at lower heating rates, presented an endothermic behaviour. For air combustion, it was concluded that all reactions were exothermic, and that the biggest amount of heat release (around 600 mW) was done at this stage. As CO₂ was mixed with air, the reaction temperature was also increased, and the amount of heat that was released was lower, due to the inert gas properties of the CO₂. For CO₂ gasification, it was seen that the behaviour was similar to pyrolysis. As there was an exothermic behaviour on high heating rates, and endothermic behaviour, but at 800°C there was a change in the behaviour of the reactions, as the CO₂ gasification reactions took place. The addition of oxygen makes the amount of heat released higher, as it could be seen that the highest amount of heat was released with air combustion. Also, higher heating rates presents higher amount of heat released, as there is a bigger flow of oxygen.

A specific heat analysis was done for all the different carrier gases. This allowed to make a qualitative approach and inferred on which different amount of components were being formed during the experiment. At the beginning it was showed that the energy that there was an endothermic behaviour, but this was due to the evaporation of the water that was content inside the biomass sample. After this evaporation, the volatiles formation was taking place approximately above 300°C, the energy to form CO and CH₄ was reached. Finally, at 360 °C, CO₂ formation energy was achieved, and the process continued to grow until the end of the test, which inferred that all the gases were being formed. As CO₂ was added to the mixture of air, the amount of energy that was released decreased, but the reaction temperatures remained between a similar range.

After this, a kinetic model was built to simulate the biomass degradation of each sample, using the mass degradation with temperature increment, and using the least-square method to fit the model to the experimentation data, using the solver tool provided by excel. The models were done with the assumption that these were first order reactions that describe the degradation of the 3 main components of the lignocellulosic biomass (hemicellulose, cellulose and lignin). The models used different mass fractions known as pseudo-components that would describe a part of the biomass decomposition reaction, until the reaction is completed. Some of the experiments required 4, 5 pseudo-components to characterize the degradation profile, in other cases, 6 pseudo-components were necessary. For the biomass degradation profiles, the models had an excellent correlation compared to the experimental data (>0.994) in all of the cases, with better correlations on the low heating rates than in the higher rates, which is given as a lack of data to approach one model to the other, and also because there at high heating rates there are several reactions occurring at the same moments, overlapping the biomass degradation stages. At lower heating rates, there can be 3

degradation stages, first hemicellulose, then cellulose and finally lignin. At high heating rates, only 2 peaks are visible, in one of them, hemicellulose, cellulose and lignin reactions are overlapping on the other one, lignin reactions are taking place. From the models it can be seen that there is a variation between the different kinetic parameters of each one of the tests. When the data was being evaluated, it was seen that the pseudo-components were not related to one component but to different mixtures between the components that made very difficult to characterize and compare each one of the parameters between them.

Finally a heat flow model was done for each DSC test, in order to simulate the behaviour of the biomass. First, It could be concluded that for low temperatures, the first behaviour was mostly endothermic, due to evaporation of moisture that was inside the biomass, which was a small fraction of the biomass (no more than 5% for almost all of the cases), followed by different behaviours according to the gas and the heating rate that was being used. It could be seen that as there was more oxygen in the mixture (bigger amount of air), there was a bigger amount of heat released, also could be confirmed when there were high heating rates, in which the biggest amount of heat released was at 100 °C/min heating rate, and at only air in the test. When the simulations were done, it was seen that there was not a good correlation between the experimental data and the model data. This could be done because of the amount of pseudo-components that there were on the model, and also because of the model that was followed to make the simulation, which had several constraints. This made that the correlation factors were not accurate and that the data from the models not to be reliable.

5.2 Recommendations

For next studies it can be recommended to separate the components of the lignocellulosic material, in order to be able to study them separately and be able to have a proper kinetic characterization and a proper heat flow modelling. It is also recommended to have a device that is able to measure properly the components of the outlet gas after the reaction has taken place. This could help to identify properly the amount of components that are being formed as the experiment is taking place that could make identify the different reactions that are taking place in the reactor. Also, a more complex method could to identify the heat analysis can be recommended, as the one that was used in this study provided correlation rates that are not describing completely and accurately the behaviour of the biomass.

ANNEX 1. HEAT FLOW MODEL FITTING

Heat flow model 50% air- 50% CO₂

	50% air- 50% CO ₂	1	2	3	4	R2
10 °C/min	Heat of reaction (kJ/g)	-39,313	5,133	-50,909	200,856	0,920
	Cp (J/K)	0,059	0,059	0,059	0,059	
20 °C/min	Heat of reaction (kJ/g)	-62,080	22,262	-52,869	244,020	0,922
	Cp (J/K)	0,045	0,045	0,045	0,045	
50 °C/min	Heat of reaction (kJ/g)	-127,958	45,812	6,562	-1,000	0,889
	Cp (J/K)	0,017	0,017	0,017	0,017	
100 °C/min	Heat of reaction (kJ/g)	-250,776	26,172	30,087	-1,000	0,912
	Cp (J/K)	0,000	0,000	0,000	0,000	

Table 18. 50%Air-50% CO₂ combustion heats of reaction model parameters for all heating rates with correlation factor.

Heat flow model 25% air- 75% CO₂

		1	2	3	4	R2
10 °C/min	Heat of reaction (kJ/g)	-39,313	5,133	-50,909	200,856	0,865
	Cp (J/K)	0,059	0,059	0,059	0,059	
20 °C/min	Heat of reaction (kJ/g)	-62,080	22,262	-52,869	244,020	0,722
	Cp (J/K)	0,045	0,045	0,045	0,045	
50 °C/min	Heat of reaction (kJ/g)	-127,958	45,812	6,562	-1,000	0,994
	Cp (J/K)	0,017	0,017	0,017	0,017	
100 °C/min	Heat of reaction (kJ/g)	-250,776	26,172	30,087	-1,000	0,995
	Cp (J/K)	0,000	0,000	0,000	0,000	

Table 19. 50%Air-50% CO₂ combustion heats of reaction model parameters for all heating rates with correlation factor.

Heat flow model pyrolysis

		1	2	3	4	5	R2
10 °C/min	Heat of reaction (kJ/g)	-0,743	-2,064	0,977	-3,443	14,578	0,84
	Cp (J/K)	0,002	0,002	0,002	0,002	0,002	
20 °C/min	Heat of reaction (kJ/g)	-1,576	-3,743	-0,043	-4,842	28,079	0,985
	Cp (J/K)	0,003	0,003	0,003	0,003	0,003	
50 °C/min	Heat of reaction (kJ/g)	-3,440	-0,920	-0,366	-3,045	-9,611	0,997
	Cp (J/K)	0,002	0,002	0,002	0,002	0,002	
100 °C/min	Heat of reaction (kJ/g)	-0,794	-0,318	-0,117	-5,115	-14,003	0,999
	Cp (J/K)	0,001	0,001	0,001	0,001	0,001	

Table 20. Pyrolysis heats of reaction model parameters for all heating rates with correlation factor.

Heat flow model CO₂ gasification

		1	2	3	4	5	6	R2
10 °C/min	Heat of reaction (kJ/g)	-2582,360	-3065,156	2074,199	-508,095	1485,118	239,899	0,768
	Cp (J/K)	0,833	0,833	0,833	0,833	0,833	0,833	
20 °C/min	Heat of reaction (kJ/g)	-154,039	-80,850	-314,495	-20,162	13,155	213,407	0,921
	Cp (J/K)	0,103	0,103	0,103	0,103	0,103	0,103	
50 °C/min	Heat of reaction (kJ/g)	51,286	9,781	57,294	-288,215	60,307	135,658	0,952
	Cp (J/K)	0,026	0,026	0,026	0,026	0,026	0,026	
100 °C/min	Heat of reaction (kJ/g)	39,581	1,227	39,901	-707,584	-0,001	303,357	0,997
	Cp (J/K)	0,023	0,023	0,023	0,023	0,023	0,023	

Table 21. CO₂ gasification heats of reaction model parameters for all heating rates with correlation factor.

6. REFERENCES

- [1] "Global Greenhouse Gas Emissions Data | Greenhouse Gas (GHG) Emissions | US EPA." [Online]. Available: <https://www.epa.gov/ghgemissions/global-greenhouse-gas-emissions-data>. [Accessed: 18-Sep-2018].
- [2] D. P. Ye, J. B. Agnew, and D. K. Zhang, "Gasification of a South Australian low-rank coal with carbon dioxide and steam: Kinetics and reactivity studies," *Fuel*, vol. 77, no. 11, pp. 1209–1219, 1998.
- [3] M.-M. F, C. T, R.-M. J, and Rodriguez. J.J, "CO₂ and steam gasification of a grapefruit skin char," *Fuel*, vol. 81, pp. 423–429, 2002.
- [4] P. Basu, *Biomass gasification, pyrolysis and torrefaction*, Second edi. Press, Academic, 2013.
- [5] S. Wang and Z. Luo, *Pyrolysis of biomass*, 1st ed. De Gruyter, 2017.
- [6] A. Akhtar, V. Krepl, and T. Ivanova, "A Combined Overview of Combustion, Pyrolysis, and Gasification of Biomass," *Energy and Fuels*, vol. 32, no. 7, pp. 7294–7318, 2018.
- [7] D. L. Klass, *Biomass for renewable energy, fuels, and chemicals*, 1st ed. San Diego: Academic Press, 1998.
- [8] S. A. Sadeek, N. A. Negm, H. H. H. Hefni, and M. M. Abdel Wahab, "Metal adsorption by agricultural biosorbents: Adsorption isotherm, kinetic and biosorbents chemical structures," *Int. J. Biol. Macromol.*, vol. 81, no. October 2017, pp. 400–409, 2015.
- [9] J. P. Diebold and B. A.V., "Overview of fast pyrolysis of biomass for the production of liquid fuels," *Dev. Thermochem. biomass Convers.*, vol. 1, pp. 5–27, 1997.
- [10] A. L. Sullivan and R. Ball, "Thermal decomposition and combustion chemistry of cellulosic biomass," *Atmos. Environ.*, vol. 47, pp. 133–141, 2012.
- [11] S. K. Sansaniwal, K. Pal, M. A. Rosen, and S. K. Tyagi, "Recent advances in the development of biomass gasification technology : A comprehensive review," vol. 72, no. December 2016, pp. 363–384, 2017.
- [12] M. A. Chawdhury, K. Mahkamov, I. M. Division, C. Sciences, and S. Road, "Development of a Small Downdraft Biomass Gasifier for Developing Countries," *J. Sci. Res.*, vol. 3, pp. 51–64, 2011.
- [13] A. Kumar, D. D. Jones, and M. A. Hanna, "Thermochemical biomass gasification: A review of the current status of the technology," *Energies*, vol. 2, no. 3, pp. 556–581, 2009.
- [14] R. P. Overend, T. A. Milne, and M. L. K., *Fundamentals of thermochemical biomass conversion*, 1st editio. Elsevier applied science publishers Ltd, 1985.
- [15] A. Gómez, W. Klose, and S. Rincón, *Pirólisis de Biomasa: Cuesco de palma de aceite*.

Universidad Nacional de Colombia. Kassel university press. 2008.

- [16] J. I. Montoya Arbeláez, F. Chejne Janna, and M. Garcia-Pérez, "Fast pyrolysis of biomass: A review of relevant aspects. Part I: Parametric study," *Dyna*, vol. 82, no. 192, pp. 239–248, 2015.
- [17] J. Shen, X. S. Wang, M. Garcia-Perez, D. Mourant, M. J. Rhodes, and C. Z. Li, "Effects of particle size on the fast pyrolysis of oil mallee woody biomass," *Fuel*, vol. 88, no. 10, pp. 1810–1817, 2009.
- [18] M. Asadullah, S. Zhang, and C. Z. Li, "Evaluation of structural features of chars from pyrolysis of biomass of different particle sizes," *Fuel Process. Technol.*, vol. 91, no. 8, pp. 877–881, 2010.
- [19] D. Chen, Y. Li, K. Cen, M. Luo, H. Li, and B. Lu, "Pyrolysis polygeneration of poplar wood: Effect of heating rate and pyrolysis temperature," *Bioresour. Technol.*, vol. 218, pp. 780–788, 2016.
- [20] A. G. Barneto, J. A. Carmona, A. Galvez, and J. A. Conesa, "Effects of the composting and the heating rate on biomass gasification," *Energy and Fuels*, vol. 23, no. 2, pp. 951–957, 2009.
- [21] E. Cetin, R. Gupta, and B. Moghtaderi, "Effect of pyrolysis pressure and heating rate on radiata pine char structure and apparent gasification reactivity," *Fuel*, vol. 84, no. 10, pp. 1328–1334, 2005.
- [22] P. T. Williams and S. Besler, "The Influence of Temperature and Heating Rate on the Slow Pyrolysis of Biomass," *Renew. Energy*, vol. 7, no. 3, pp. 233–250, 1996.
- [23] A. Demirbas, "Effects of temperature and particle size on bio-char yield from pyrolysis of agricultural residues," *J. Anal. Appl. Pyrolysis*, vol. 72, no. 2, pp. 243–248, 2004.
- [24] J. Zhang, J. Liu, and R. Liu, "Effects of pyrolysis temperature and heating time on biochar obtained from the pyrolysis of straw and lignosulfonate," *Bioresour. Technol.*, vol. 176, pp. 288–291, 2015.
- [25] M. Balas, M. Lisy, and O. Stelcl, "The Effect of Temperature on the Gasification Process," *Acta Polytech.*, vol. 52, no. 4, pp. 7–11, 2012.
- [26] H. C. Buttermann and M. J. Castaldi, "CO₂ as a carbon neutral fuel source via enhanced biomass gasification," *Environ. Sci. Technol.*, vol. 43, no. 23, pp. 9030–9037, 2009.
- [27] M. Jeremiáš *et al.*, "Gasification of biomass with CO₂ and H₂O mixtures in a catalytic fluidised bed," *Fuel*, vol. 210, no. September, pp. 605–610, 2017.
- [28] Y. Cheng, Z. Thow, and C. H. Wang, "Biomass gasification with CO₂ in a fluidized bed," *Powder Technol.*, vol. 296, pp. 87–101, 2016.
- [29] N. Prakash and T. Karunanithi, "Kinetic Modeling in Biomass Pyrolysis - a review," *J. Appl. Sci.*

- Res.*, vol. 4, no. 12, pp. 1627–1636, 2008.
- [30] F. Thurner and U. Mann, “Kinetic investigation of wood pyrolysis Kinetic Investigation of Wood Pyrolysis,” *Ind. Eng. Chem. Process Des. Dev.*, vol. 20, no. 3, pp. 482–488, 1981.
- [31] F. J. Kilzer and A. Broido, “Speculations on the nature of cellulose pyrolysis,” *Pyroynamics*, vol. 2, no. April 1964, pp. 151–163, 1965.
- [32] G. Várhegyi, E. Jakab, and M. J. Antal, “Is the Broido-Shafizadeh Model for Cellulose Pyrolysis True? †,” *Energy and fuels*, no. 8, pp. 1345–1352, 1994.
- [33] C. Branca and C. Di Blasi, “Kinetics of the isothermal degradation of wood in the temperature range 528–708 K,” *J. Anal. Appl. Pyrolysis*, vol. 67, no. 2, pp. 207–219, 2003.
- [34] R. Murillo *et al.*, “Kinetic Model Comparison for Waste Tire Char Reaction with CO₂,” *Ind. Eng. Chem. Res.*, vol. 43, no. 24, pp. 7768–7773, 2004.
- [35] M. Ishida and C. Y. Wen, “Comparison of zone-reaction model and unreacted-core shrinking model in solid-gas reactions- I Isothermal analysis,” *Chem. Eng. Sci.*, vol. 26, pp. 1031–1041, 1971.
- [36] C. D. Georgakis, W. Chang, and J. Szeckely, “A changing grain size model for solid-gas reactions,” *Chem. Eng. Sci.*, vol. 34, pp. 1072–1075, 1979.
- [37] S. K. Bhatia and D. D. Perlmutter, “A random pore model for fluid-solid reactions: I. Isothermal, kinetic control,” *AIChE J.*, vol. 26, no. 3, pp. 379–386, 1980.
- [38] Nedelchev, N and D. T. Zvezdova, “NEW APPROACH TO DIFFERENTIAL METHODS FOR NON-ISOTHERMAL KINETIC STUDIES,” *Oxid. Commun.*, vol. 36, no. 4, pp. 1175–1194, 2013.
- [39] M. H. Abbasi and R. E. Kahrizangi, “Evaluation of reliability of Coats-Redfern method for kinetic analysis of non-isothermal TGA,” *Trans.Nonferrous Met. Soc. China*, pp. 217–221, 2008.
- [40] J. G. Huelva, “Thermochemical Characterization of Biomass Modelling combustion and pyrolysis kinetic,” *Inst. Super. Tec.*, no. November, 2017.
- [41] D. D. Pokwiczal, “Thermochemical Conversion of Biomass – Kinetics , Gasifier Modeling and Design,” *Inst. Super. Tec.*, no. February, pp. 1–74, 2017.
- [42] H. L. Friedman, “Kinetics of thermal degradation of char-forming plastics from thermogravimetry. Application to a phenolic plastic,” *J. Polym. Sci. Part C Polym. Symp.*, vol. 6, no. 1, pp. 183–195, 1964.
- [43] H. E. Kissinger, “Reaction Kinetics in Differential Thermal Analysis,” *Anal. Chem.*, vol. 29, no. 11, pp. 1702–1706, 1957.

- [44] M. E. Brown, "Introduction to Thermal Analysis: Techniques and Applications," *Mineralogical Magazine*, vol. 53, no. 373, pp. 1–207, 1989.
- [45] Y. Haseli, J. A. Van Oijen, and L. P. H. De Goeij, "Modeling biomass particle pyrolysis with temperature-dependent heat of reactions," *J. Anal. Appl. Pyrolysis*, vol. 90, no. 2, pp. 140–154, 2011.
- [46] A. Koufopoulos, C and N. Papayannakos, "Modelling of the pyrolysis of biomass particles. Studies on kinetics, thermal and heat transfer effects," *Can. J. Chem. Eng.*, vol. 69, pp. 907–915, 1991.
- [47] S. Vyazovkin *et al.*, "ICTAC Kinetics Committee recommendations for collecting experimental thermal analysis data for kinetic computations," *Thermochim. Acta*, vol. 590, pp. 1–23, 2014.
- [48] H. Yang, R. Yan, H. Chen, D. H. Lee, and C. Zheng, "Characteristics of hemicellulose, cellulose and lignin pyrolysis," *Fuel*, vol. 86, no. 12–13, pp. 1781–1788, 2007.